Ectopic expression of Cripto-1 in transgenic mouse liver promotes hepatocyte proliferation, and causes the altered expression of hepatocarcinogenesis-related genes

Yu Liu
Southern Medical University
Yan-Qing Li
Central Hospital of Xuhui District
Jun-Shuang Jia
Southern Medical University
Wen-Tao Zhao
Southern Medical University
Fang Wei
Southern Medical University
Jia-Hong Wang
Southern Medical University
Guan-Qi Dai
Southern Medical University
Shi-Hao Huang
Southern Medical University
Yu-Cai Wang
Southern Medical University
Yong-Long Li
Southern Medical University
Xiao-Yan Li
Southern Medical University
Liu-Xin Han
The third people's hospital of Kunming
Dong Xiao
Southern Medical University
Kang Xu
Sun Yat-sen University
Xiaolin Lin (zheyilxl886@126.com)
Southern Medical university https://orcid.org/0000-0001-7457-9017

Research

Keywords: Cripto-1 (CR-1), hepatocellular carcinoma (HCC), transgenic mice, hepatocarcinogenesis

Posted Date: March 24th, 2020

DOI: https://doi.org/10.21203/rs.3.rs-18969/v1

Ectopic expression of Cripto-1 in transgenic mouse liver promotes hepatocyte proliferation, and causes the altered expression of hepatocarcinogenesis-related genes

Yu Liu[1,2,†], Yan-Qing Li[3,†], Jun-Shuang Jia[1,†], Wen-Tao Zhao[1,4,†], Fang Wei[1], Jia-Hong Wang[1], Guan-Qi Dai[1], Shi-Hao Huang[1], Yu-Cai Wang[1], Yong-Long Li[1,2], Xiao-Yan Li[1,2], Liu-Xin Han[5], Dong Xiao[1,2,*], Kang Xu[6,7,*], Xiao-Lin Lin[1,*]

[1]Guangdong Provincial Key Laboratory of Cancer Immunotherapy Research and Guangzhou Key Laboratory of Tumour Immunology Research, Cancer Research Institute, School of Basic Medical Science, Southern Medical University, Guangzhou 510515, China

[2]Institute of Comparative Medicine & Laboratory Animal Center, Southern Medical University, Guangzhou 510515, China

[3]Department of Hematology, Central Hospital of Xuhui District, Shanghai 20003, China

[4]Department of Medical Oncology, The Third Affiliated Hospital of Kunming Medical University (Tumour Hospital of Yunnan Province), Kunming 650118, China

[5]The third people's hospital of Kunming, Kunming 650041, China

[6]Department of General Surgery, Sun Yat-sen Memorial Hospital, Sun Yat-sen University, Guangzhou, China

[7]Guangdong Provincial Key Laboratory of Malignant Tumour Epigenetics and Gene Regulation, Sun Yat-Sen Memorial Hospital, Sun Yat-Sen University, Guangzhou, China

Running title:

Increased hepatocyte proliferation and hepatocarcinogenesis-related genes deregulated in hepatocyte-targeted Cripto-1 transgenic mouse liver

---

[†]These authors contributed equally to this work.

*Corresponding authors: **Xiao-Lin Lin**, zheyilxl886@126.com;

Kang Xu, xukang1995@yahoo.com; **Dong Xiao**, Xiao_d@hotmail.com and xiaodong@smu.edu.cn.

Abstract

Background: Embryonic gene Cripto-1 (CR-1) is not detected or expressed at low levels in normal adult tissues, however, is re-expressed in numerous tumors, including hepatocellular carcinoma (HCC) and CR-1 transgene overexpression led to mammary epithelial hyperplasia and adenocarcinoma, which prompted us to investigate whether hepatocyte-specific overexpression of CR-1 in transgenic mice can initiate hepatocarcinogenesis.

Methods: Semi-quantitative RT-PCR, qRT-PCR, Western blotting or immunohistochemical staining were employed to detected CR-1 mRNA transcript or CR-1 expression in HCC tissue specimens. Combined use of CR-1 transgenic mice, microarray, 2/3 partial hepatectomy (PHx), and TCGA and GEO database examined the functions of CR-1 in initiate hepatocelluar carcinogenesis.

Results: Here we firstly provided the direct evidence that a truncated 1.7-kb mRNA transcript from CR-1 geneis dominantly expressed in HCC specimens, suggesting the importance of short CR-1 mRNA form in HCC progression.We found that CR-1 is frequently upregulated in HCC specimens. Hepatocyte-specific overexpression of CR-1 in transgenic mice promoted hepatocyte proliferationafter 2/3 PHx, CR-1 positively regulated HCC cell proliferation and invasion in vitro, and CR-1 overexpression promoted tumour growth of HCC cells in nude mice. In this study, we demonstrated that CR-1 transgenic overexpression in transgenic liver abnormally activated downstream pathways (i.e., AKT, Wnt/β-catenin, Stat3, MAPK/ERK, JNK, TGF-β and Notch) and led to the deregulated expression profile of genes, including up-regulated genes (i.e., CD5L, S100A8, S100A9, Timd4, Orm2, Orm3, Saa1, Saa3, Itih3, Itih4, Ly6e, IGHG1, IGHG2B and Vnn3) and down-regulated genes (i.e.,PDK4, DMBT1, G0S2, Plk2, Plk3, Gsta1 and Gsta2), all of which are key regulators of cellular proliferation, inflammation response, cellular malignant transformation, hepatocarcinogenesis or HCC progression, however, there were no histological signs of precancerous lesions, hepatocyte dysplasia and HCC formation in livers samples from 3-, 6- or 8-month-old RCLG/Alb-Cre transgenic mice, suggesting that the constitutive expression of CR-1 alone is not sufficient to promote hepatocarcinogenesis, unless other factors, i.e., a second hit, is present.

Conclusions: Taken together, we provide the first in vivo genetic evidence that CR-1 overexpression in transgenic mouse liver promotes hepatocyte proliferation after 2/3 PHx, and causes the deregulated molecular alterations involved in HCC oncogenesis, however, these abnormally molecular alterations are not sufficient to initiate hepatocarcinogenesis in mice.

Keywords: Cripto-1 (CR-1), hepatocellular carcinoma (HCC), transgenic mice, hepatocarcinogenesis

Background

Hepatocellular carcinoma (HCC) is one of the most common cancer types worldwide with an extremely poor prognosis[1]. Among the primary liver cancers, HCC represents the major histological subtype, accounting for 70-85% of the total cases[1]. The 5-year postoperative recurrence rate for this disease is greater than 60%, and the median 5-year survival rates after repeat hepatectomy, ablation and transarterial chemoembolization (TACE) were 35.2, 48.3 and 15.5 percent, respectively[2, 3]. HCC results from a combination of environmental factors such as cytotoxic and DNA-damaging chemicals, hepatitis B virus (HBV) infection and the accumulation of generalized and specific genetic alterations[4-11]. Although there is mounting evidence that the abnormal alterations of some signal pathways, such as Wnt/β-catenin, PI3K/AKT/GSK-3β, MAPK/ERK, TGFß/BMP, mTOR and Stat3, and genes, such as HBx, p53, c-Myc, $p16^{INK4A}$, K-Ras, APC, BRCA2, CDK2, cyclin E1, cyclin D, cyclin A and p38γ, can initiate HCC in mice [6, 8-10, 12-19], the molecular pathogenesis of HCC is still under intense investigation.

Cripto-1 (CR-1) is a member of the epidermal growth factor (EGF)-Cripto-1/fibroblast growth factor related ligand (FRL1)/Criptic (EGF-CFC) protein family, which contains an EGF-like domain and a cysteine-rich region called the Cripto-1/FRL1/Cryptic (CFC) domain (Cripto-1 in humans, FRL1 in Xenopus, and Cryptic in mice)[20-26]. CR-1 gene is a key player in this complex scenario[20-27]. CR-1 is identified to exert essential biological functions during embryogenesis, and is considered a marker of undifferentiated embryonic stem cells[20-26]. It is indispensable in coordinating primitive streak formation, mesoderm and endoderm specification as well as anterior and posterior (A/P) axis orientation[27-31]. CR-1 is not detected or expressed at low levels in normal adult tissues[20-27], but is re-expressed at a high frequency in a number of different types of human carcinomas, such as lung, breast, colon, and stomach cancers, and nasopharyngeal carcinoma[21, 24, 32-37]. Emerging evidence has clearly demonstrated that the inappropriate activation of embryonic regulatory genes such as Oct4 contributes to cell malignant transformation and oncogenes is in adult tissues[38-40]. Like Oct4, another example of such a case is the embryonic gene CR-1. CR-1 transgene overexpression in MMTV-CR-1 or WAP-CR-1 transgenic mouse mammary gland

caused mammary hyperplasia and adenocarcinoma[26, 41], and the development of leiomyosarcoma of the uterus in MMTV-CR-1 transgenic mice[42]. CR-1 exerts its pro-tumorigenic influences on colorectal cancer[43], breast cancer[44], melanoma[45], esophageal squamous cell carcinoma[46], cervical carcinoma[47] and nasopharyngeal carcinoma[35], suggesting the oncogenic roles of CR-1. Therefore, CR-1 is a multifunctional modulator involved in embryogenesis, oncogenesis and cancer progression[20-27].

Of note, several lines of evidence have indicated that CR-1 is associated with HCC progression[48-50]. Elevated expression of CR-1 contributes to aggressiveness and poor prognosis of HCC, and CR-1/AFP expression could be a potential prognostic biomarker for survival in HCC patients[49]. The serum CR-1 level was significantly higher in patients with cirrhosis, chronic hepatitis or HCC than volunteer controls and it was also significantly higher in HBV-related HCC than HCV-related HCC[50]. CR-1 positively regulated the proliferation, tumorigenicity, migration, invasion and chemoresistance of HCC cells[48]. In addition, CR-1 contributes to stemness in HCC by stabilizing Dishevelled-3 and activating Wnt/β-catenin pathway[48]. Together, the aforementioned findings indicate that CR-1 exerts its pro-tumorigenic influences on HCC. However, a direct evidence that CR-1 as oncogene can also initiate hepatocarcinogenesis is not obtained experimentally in transgenic mice.

Given that the enforced expression of CR-1 transgene in transgenic mouse mammary gland caused mammary hyperplasia and adenocarcinoma[41, 42], and CR-1 exerts its pro-tumorigenic effects on HCC[48-50], the present study aimed to investigate whether hepatocyte-specific overexpression of CR-1 in transgenic mice can initiate hepatocarcinogenesis.

Materials and Methods

Cell lines and cell culture

The human HCC cell lines, BEL-7402 and HepG2, were purchased from the Cell Bank of the Chinese Academy of Sciences (Shanghai, China). HEK293T cells were obtained from the

American Type Culture Collection (ATCC). These cells were cultured in Dulbecco's modified Eagle's medium (DMEM) (high glucose) supplemented with 10% fetal bovine serum (FBS), 1% non-essential amino acids (NEAA), 1 mM L-glutamine and 1 mM sodium pyruvate in a humidified incubator with 5% CO_2 at 37℃.

Clinical specimens

Fresh primary HCC specimens and tumor-adjacent noncancerous tissues of the HCC were collected from Sun Yat-sen Memorial Hospital, Sun Yat-sen University (Guangzhou, China) with informed consent under institutional review board-approved protocols. The inclusion criteria of HCC cases were based on (1) a clear pathological diagnosis of HCC, (2) no anticancer treatment before surgery. Total RNA was extracted from the fresh-frozen specimens, and used for RT-PCR and qRT-PCR analysis, while total protein extracted from these fresh-frozen samples was employed in Western blot analysis. The formalin-fixed paraffin-embedded HCC samples were prepared from the above-mentioned fresh-frozen specimens by us. Ethical approval was given by the Medical Ethics Committee of Southern Medical University.

Total RNA isolation, reverse transcription, RT-PCR and quantitative real-time PCR (qRT-PCR)

Total RNA isolation, reverse transcription, RT-PCR and qRT-PCR were performed as previously described[3, 27, 51-59]. For RT-PCR analysis, CR-1-specific oligo nucleotide primer sequences were chosen to amplify two distinct regions according to the CR-1 cDNA sequence[60, 61]. The oligo nucleotide primers are: UN-A forward primer (nucleotides 375–398) ： 5′-ACCTGGCCTTCAGAGATGACAGCA-3′, UN-B reverse primer (nucleotides 656–680): 5′-ATGCCTGAGGAAAGCAGCGGAGCT-3′ and UN-D forward primer (nucleotides 248–266): 5′-AAAGCTATGGACTGCAGGA-3′ (Fig. 1A). The primer couples UN-D/UN-B and UN-A/UN-B yield PCR products of 432bp and 305bp, respectively (Fig. 1A). GAPDH was used as a control, and the primers used for the amplification of GAPDH gene are listed in Table S1.

The primers used in qRT-PCR assays were listed in Table S2 and Table S3. GAPDH was used

as an endogenous control. All samples were normalized to internal controls and fold changes were calculated through relative quantification ($2^{-\triangle\triangle Ct}$).

Western blot analysis

Western blot were performed as previously described[3, 27, 51-59]. The blots were probed with the indicated primary antibodies, followed by HRP (horseradish peroxidase)-labeled secondary antibodies. The hybridization signal was detected using enhanced chemiluminescence (ECL). GAPDH or β-actin was used as a loading control. The primary antibodies used in this study were shown in Table S4.

Histological analysis and immunohistochemistry (IHC)

Histological analysis and immunohistochemical staining were performed as previously described[3, 27, 51-59]. The antibodies and conditions used are summarized in the Table S4.

Lentivirus production and transduction

Human CR-1 lentiviral shRNA vector (designated pLV-shCR-1) and the empty lentiviral vector expressing scrambled shRNA (designated pLV-shSCR), and lentiviral CR-1 expression vector (designated pLV-CR-1) and its empty lentiviral vector (designated pLV-con) were generously provided by Prof. Peter C. Gray (The Salk Institute for Biological Studies, USA.)[62]. The lentiviral packaging plasmids psPAX2 and pMD2.G were kindly provided by Dr. Didier Trono (University of Geneva, Geneva, Switzerland). To generate stable cell lines, recombinant lentiviruses (namely LV-con, LV-CR-1, LV-shSCR and LV-shCR-1) were generated as previously described[56, 63], and subsequently used to infect BEL-7402 and HepG2 cells.

Colony formation assay

Colony formation assay were performed as previously described[3, 55].

Transwell migration assay and Boyden invasion assay

Transwell migration assay and Boyden invasion assay were performed as described previously[3, 55, 58].

Tumor xenograft in nude mice

Female BALB/c nude mice aged 3 to 4 weeks were purchased from the Medical Laboratory Animal Center of Guangdong Province. Vector- or CR-1-expressing BEL-7402 cells (1×10^6 cells) were subcutaneously injected into the left or right dorsal thigh of mice (n=7), respectively. The tumor volumes were measured every 2 days using a caliper slide rule. Tumor volumes were calculated as follows: volume=$(D\times d^2)/2$, where D meant the longest diameter and d meant the shortest diameter. On day 20 after cancer cell implantation, mice were sacrificed, and tumors were dissected, weighed and fixed overnight in 4% paraformaldehyde, dehydrated, paraffin-embedded, sectioned. The animal experiments were carried out in strict accordance with the recommendations in the Guide for the Care and Use of Laboratory Animals of the Southern Medical University. The animal protocol was approved by the Committee on Ethics of Animal Experiments of the Southern Medical University. All surgery was performed under sodium pentobarbital anesthesia, and all efforts were made to minimize suffering of animals.

Production of the RCLG transgenic mice

The pCI-cripto-1[64] and pCAG-RLG[65, 66] vectors were generously provided by Dr. David S. Salomon (Center for Cancer Research, National Cancer Institute, USA) and Prof. Manuela Martins-Green (University of California, USA), respectively. A 600 bp fragment containing the Cripto-1 cDNA was amplified from the pCI-cripto-1 plasmid using PCR[64], after which the cDNA was then cloned into the *Sma* I site of the pCAG-RLG[65, 66] parental vector to generate the RCLG transgenic construct, which is designated as pCAG-RCLG (Fig. S1A). The vector was characterized molecularly by PCR, enzyme digestion analysis and DNA sequencing (data not shown).

RCLG transgenic mice were generated by microinjecting DNA into the pronuclei of fertilized embryos using standard techniques that have previously been described[67]. The FVB/N strain was used as the source of embryos for micromanipulation and the subsequent breeding trials. All of the transgenic lines were created on the FVB/N genetic background. For the microinjection, the 9.436 kb fragment of RCLG transgene (Fig. S1A) was released from

the pCAG-RCLG vector backbone by digestion with *Ssp* I and *Sfi* I, and was subsequently isolated and purified using the QIA quick gel extraction kit (Qiagen, Germany). The fragment was diluted to a final concentration of 2 μg/ml in DNA injection buffer (10 mM Tris/0.1 mM EDTA, pH 7.4) and then microinjected into the pronuclei of fertilized FVB/N embryos. About 20~30 injected eggs were transferred into the oviducts of one pseudopregnant ICR mouse and developed to term. Two to three days after birth, the offspring were screened to identify potential RCLG transgenic founders using an mRFP assay by the IVIS Lumina Ⅱ imaging system (Xenogen Corp., Alameda, CA, USA). The results of this assay were subsequently confirmed with PCR-based genotyping.

Whole-animal (*in vivo*) and organ (*ex vivo*) fluorescence imaging

The procedure for whole-animal and organ mRFP (monomeric red fluorescent protein) fluorescence imaging via using stereo fluorescence microscope (Nikon, AZ100) or the Xenogen IVIS Lumina Ⅱ Imaging System was previously fully described[27, 52, 55, 68-70].

***In vivo* and ex vivo optical imaging of firefly luciferase (Luc) activity**

RCLG mice were crossed to homozygous Alb-Cre mice (B6.Cg-Tg(Alb-cre)21Mgn/J) (obtained from Model Animal Research Center of Nanjing University) to generate RCLG/Alb-Cre double transgenic mice, in which Luc expression was activated in liver-restricted pattern, as determined by the non-invasive *in vivo* bioluminescence imaging. Bioluminescence was measured non-invasively using the IVIS Lumina Ⅱ imaging system. The protocols for whole-animal (*in vivo*) and dissected organ (ex vivo) bioluminescence imaging to detect Luc activity by the IVIS system were previously well described[3, 27, 52, 55, 68-70].

Genotype analysis by PCR

PCR was performed on tail genomic DNA to further identify RCLG/Alb-Cre double transgenic mice. The sequences of the forward primer (FP) and reverse primer (RP) specific for Luc gene and Cre gene were described in Table S5.

mRNA microarray analysis

Expression microarray analysis was carried out with commercially available 32K mouse genome array (Capital Bio Corp., Bejing, China). Total RNA samples were extracted from the liver of RCLG/Alb-Cre transgenic mice and control mice using TRIzol reagent (TaKaRa). All the hybridization procedures and data analysis were performed by Capital Bio Corp. (Bejing, China). Briefly, total RNA was used to synthesize cDNA in an *in vitro* transcription reaction, and then cDNA was fluorescently labeled by Cy5-dCTP or Cy3-dCTP (GE Healthcare Cat. No. PA 55021/PA 53021) with Klenow enzyme. Labeled cDNA was then hybridized to 32K mouse genome arrays. Hybridization signals were scanned with a Lux-Scan 3.0 scanner (Capital Bio Corp., Bejing, China). The resultant images were digitized with Lux-Scan 3.0 image analyzer software (Capital Bio Corp., Bejing, China). The microarray data were deposited in a database (ArrayExpress, GEO) with accession number GSE64255.

Statistical analysis

The data were presented as mean ± SEM. Statistical analysis was performed using a SPSS 13.0 software package and Graphpad 5.0 software. Two-tailed Student's t test was used for comparisons of two independent groups. Values are statistically significant at $^{*}P<0.05$, $^{**}P<0.01$ and $^{\#}P<0.001$.

Results

1. The short form CR-1 mRNA is dominantly expressed in HCC cell lines and tissue specimens

As shown in Fig. 1A, both the longer 2-kb CR-1 mRNA transcript [i.e., full-length CR-1 (FL-CR-1) mRNA] and the shorter 1.7-kb CR-1 mRNA transcript [i.e., short form CR-1 (SF-CR-1) mRNA] are expressed in mammalian cells and tissues[60, 61]. To determine and quantify the full-length CR-1 mRNA within the total CR-1 transcript in human HCC cell lines and HCC clinical tissue specimens, we employed a full length CR-1 specific primer set (UND/UNB) and total CR-1 primer set (UNA/UNB) that reacts to FL-CR-1 and SF-CR-1 (Fig. 1A), respectively. RT-PCR analysis revealed that six different HCC cell lines (i.e., QGY7701, HepG2, Hep3B, SK-Hep-1, SNU-182 and SNU-387 cells expressed both a complete,

full-length 2.0-kb mRNA transcript and a truncated 1.7-kb mRNA transcript from the human CR-1 gene (Fig. 1B). As indicated in Fig. 1C, semi-quantitative RT-PCR assay displayed that 62% of the total CR-1 transcripts were represented by full-length CR-1 in SK-Hep-1 cells. In contrast, in HCC cell lines (i.e., QGY7701, HepG2, Hep3B, SNU-182 and SNU-387 cells full-length CR-1 transcript expression was significantly lower (less than 16%) than SK-Hep-1 cells, suggesting that the majority of CR-1 transcripts represent the SF-CR-1 in QGY7701, HepG2, Hep3B, SNU-182 and SNU-387 cells (Fig. 1C).

Next, using the RT-PCR assay described above, we analysed 24 pairs of adjacent non-tumorous liver tissue biopsies and HCC clinical specimens to determine which form of CR-1 mRNA transcript is expressed. RT-PCR analysis revealed that adjacent non-tumorous liver tissue biopsies and HCC clinical specimens showed the two bands (corresponding to the shorter CR-1 mRNA form and the full length CR-1 mRNA form) of the expected size derived from the longer mRNA species (CR-1) (Fig. 1D, F). Furthermore, the full-length CR-1 transcript expression in HCC tissue specimens (n=18, 75%) and adjacent non-tumorous liver tissues (n=22, 92%) was significantly lower (less than 20%) (Fig. 1E, G), suggesting that the majority of CR-1 transcripts represent the SF-CR-1 in the above-mentioned samples. Collectively, the short form CR-1 mRNA is dominantly expressed in HCC cell lines, adjacent non-tumorous liver tissues and HCC clinical tissue specimens.

2. CR-1 is frequently upregulated in HCC tissue specimens

To evaluate the potential functions of CR-1 in HCC progression, RT-PCR assay and qRT-PCR assay were performed to quantify the transcript abundance of CR-1 in freshly collected HCC tissues and freshly collected non-cancerous liver tissue biopsies. Our results from qualitative (Fig. 1A) and semi-quantitative (Fig. 2B) RT-PCR assays revealed that the expression of CR-1 mRNA transcripts was markedly upregulated in HCC tissue biopsies, compared with adjacent non-tumorous liver tissues. Consistent with the data obtained from RT-PCR assay (Fig. 2A, B), qRT-PCR assay showed that the average CR-1 mRNA expression level was significantly higher in the HCC specimens than in the non-tumour liver tissues (Fig. 2C). Additionally, TCGA datasets revealed that the up-regulated expression of CR-1 was observed in HCC tissues as

compared with adjacent non-tumorous liver tissues (Fig. 2D). Collectively, the RT-PCR analysis, qRT-PCR analysis TCGA datasets clearly showed that the increased expression of CR-1 mRNA transcripts was frequently detected in HCC clinical tissue biopsies.

The protein expression levels of CR-1 were further evaluated in additional 9 paired human HCC specimens, 4 unpaired human HCC specimens and 1 normal liver tissue by Western blotting (Fig. 2E), confirming the observation that the protein levels of CR-1 was obviously upregulated in HCC specimens. Moreover, tissue array containing the pairs of HCC samples was also examined by immunohistochemical staining with a specific antibody against CR-1. The resulting data showed that CR-1 was significantly overexpressed in HCC specimens as compared with that of corresponding noncancerous livers (Fig. 2F, G). Therefore, the results from Western blotting and IHC staining demonstrate that CR-1 upregulation is more frequently occurred in HCC tissue biopsies than their non-cancerous counterparts.

3. Generation of RCLG transgenic mice

To realize the above-mentioned purposes and attain further insight into the cell/tissue-specific and/or developmental stage-specific roles of CR-1 *in vivo*, we want to produce transgenic mice that could conditionally overexpress human CR-1 transgene mediated by Cre/*lox* P system (Fig. S1A). To understand the roles and mechanisms of CR-1 in oncogenesis, CR-1 transgenic mice, designated as RCLG transgenic mice, were successfully generated in this study (Fig. S1)[27]. Thus, we gained two founder animals (referred to as $190^{\#}$ and $220^{\#}$) that expressed strongly mRFP and were normal in phenotype (Fig. S1B). In general, RCLG transgenic mice were viable and fertile, and manifested no gross behavioral or phenotypic abnormalities.

We next determined the expression pattern of the mRFP transgene in organs taken from RCLG transgenic mice. Red fluorescence was detected in tissue/organ samples including heart, liver, spleen, lung, kidney, brain, testis, intestine, thymus, and pancreas isolated from the transgenic positive mice, but not in control littermates (Fig. S2). Additionally, the heart, liver, lung, kidney, brain, testis, intestine, thymus, and pancreas showed strong red

fluorescence, while the spleen demonstrated relatively weaker fluorescence signals (Fig. S2). In summary, all tissues exhibited mRFP expression, indicating ubiquitous expression of the transgenic cassette.

Furthermore, the sections of the tissues revealed that most cells of heart, brain, lung, kidney, liver, stomach, intestine and testis taken from RCLG transgenic mice were positive for mRFP (Fig. S3). But because some cells did not appear to be RFP positive, this mouse line may not be useful for studying all tissues or all cell types.

4. Liver-specific overexpression of CR-1 in transgenic mice mediated by Cre/*lox* P system

To further determine whether or not CR-1 overexpression can initiate liver oncogenesis, we crossed heterozygous RCLG transgenic mice with homozygous Alb-Cre mice in which Cre is under the control of the liver-specific albumin (Alb) promoter[71] to generate RCLG/Alb-Cre double transgenic mice in which CR-1 and Luc transgene expression was expected to be activated in liver-restricted manner (Fig. S4A), as determined by the noninvasive *in vivo* bioluminescence imaging (Fig. S4B, C, E, F), PCR-based genotyping (Fig. S4D), RT-PCR (Fig. S4G) and Western blotting (Fig. S4H), respectively. Whole-animal bioluminescence imaging indicated that Luc activity in the liver of RCLG/Alb-Cre transgenic mice could be detected in mRFP-positive newborn offspring (Fig. S4B, C) which were confirmed by PCR-based genotyping (Fig. S4D), and adult mouse (Fig. S4E), suggesting the successful activation of Luc expression mediated by Alb-Cre. Organ-specific bioluminescence imaging showed that Luc activity could be assayed in liver (Fig. S4F), but not in other organs obtained from Luc-positive mouse [genotype: RCLG/Alb-Cre; marked by pound (#); shown in Fig. S4E], while Luc activity could not be detected in all of organs obtained from Luc-negative mouse shown in Fig. S4E (data not shown). RT-PCR using RNA extracted from the liver of Luc-positive and Luc-negative mice exhibited a significant increase in the levels of CR-1 transgene (Fig. S4G), as further verified by Western blotting(Fig. S4H). Summarily, these data lead us to conclude that liver-specific overexpression of CR-1 transgene in transgenic mice mediated by Cre/lox P system is realized successfully.

5. Gross morphology, appearance and histopathology of RCLG/Alb-Cre transgenic livers

To determine the functional consequences of CR-1 transgene overexpression in mouse liver, comparisons were made between RCLG/Alb-Cre mice and control mice. The enforced expression of human CR-1 in the liver of RCLG/Alb-Cre mice did not alter the final body weight (Fig. 3A, B) and liver weight (Fig. 3C) of RCLG/Alb-Cre mice at different ages. No evident difference in gross morphology and appearance of mice (Fig. 3A) and the corresponding livers (Fig. 3D) was found between control and RCLG/Alb-Cre mice at the age of 3, 6 and 8m. Moreover, no notably histopathological changes, such as abnormal liver structure, a significant increase in the number of mitotichepatocytes, liver cell dysplasia and subsequent malignant transformation, etc, were observed in the histological images of H&E staining of liver sections from RCLG/Alb-Cre mice at the age of 3, 6 and 8m, compared with control littermates (Fig. 3E).There is no significant differences in the percentage of Ki67-positive nuclei in the hepatocytes between control and RCLG/Alb-Cre mice at the age of 3, 6 and 8m (Fig. 3F). Here, we provide the critical *in vivo* genetic evidence that the enforced expression of CR-1 transgene in mouse hepatocytes alone is not sufficient for hepatocyte hyperplasia, and hepatocellular carcinogenesis in the liver of RCLG/Alb-Cre mice.

6. Increased hepatocyte proliferation in CR-1-overexpressing hepatocytes after 2/3 PHx

To determine if further CR-1 overexpression might enhance liver regeneration, we performed after 2/3 partial hepatectomy (2/3 PHx) in both RCLG/Alb-Cre mice and littermate controls (Fig. 3), and liver tissue samples were collected on days 1, 1.5, 2 and 3 after 2/3 PHx. Liver regeneration was evaluated in the RCLG/Alb-Cre and control mice by using Ki67 staining. Ki67 immunohistochemistry results demonstrated that in RCLG/Alb-Cre mice, there was abundant hepatocyte proliferation 1, 1.5, 2 and 3 days after PHx, and this was demonstrated by the percentage of Ki67-positive nuclei (Fig. 3G, H). Altogether, these data demonstrate that CR-1 overexpression in mouse liver enhances hepatocyte proliferation after hepatectomy. Altogether, these data demonstrate that CR-1 overexpression is permissive of enhanced growth after injury.

7. CR-1 positively regulates HCC cell proliferation, migration and invasion *in vitro*

Given that the data (Fig. 2) illustrated that CR-1 is significantly up-regulated in HCC tissue specimens, we suspected that CR-1 may play an essential role in HCC progression, which prompted us to perform gain-of-function and loss-of-function experiments to further explore the effects of CR-1 on HCC cell growth, migration and invasion by colony formation assay, transwell migration assays and Boyden chamber invasion assays, respectively. The CR-1 transgene was successfully over-expressed in BEL-7402 and HepG2 cells (Fig. 4A), while the shRNA-CR-1 specifically knocked down endogenous CR-1 protein expression in both BEL-7402 and HepG2 cells (Fig. 4B). Colony formation assay (Fig. 4C and Fig. S5) revealed that CR-1 overexpression resulted in significantly increased HCC cell growth. Conversely, colony formation assays also demonstrated that knockdown of endogenous CR-1 by RNA interference (RNAi) markedly reduced the proliferation of BEL-7402 and HepG2 cells (Fig. 4C and Fig. S5). Furthermore, transwell migration assays and Boyden chamber invasion assays showed that CR-1 overexpression enhanced BEL-7402 and HepG2 cells migration and invasion (Fig. 4D, E and Fig. S6), while CR-1 silencing by RNAi inhibited HCC cell migration and invasion (Fig. 4D, E and Fig. S6). Summarily, CR-1 positively modulated HCC cell proliferation, migration and invasion *in vitro*.

8. CR-1 overexpression promotes tumour growth of HCC cells *in vivo*

To further confirm the growth-promoting effects of CR-1 on HCC cells *in vivo*, the subcutaneous tumour xenograft experiments were performed in nude mice. Significantly larger tumors were observed in mice injected with CR-1-overexpressing 7402 cells than in the mice injected with empty vector-transduced HCC cells (Fig. 4F). The tumor volume (Fig. 4H), tumor size (Fig. 4G) and tumor weight (Fig. 4I) were significantly larger in tumors induced by CR-1-expressing cells compared with tumors induced by vector-expressing cells. In addition, the results of immunohistochemical analysis revealed that tumours formed from the CR-1-overexpressing cells contained a markedly increased number of 5-bromo-2'-deoxyuridine (BrdU)-positive cells, compared with control (Fig. 4J, K). Taken together, these findings demonstrate that CR-1 can promote *in vivo* tumorigenicity of HCC

cells.

9. Altered molecular pathways in the livers of RCLG/Alb-Cre transgenic mice

We next explored the molecular pathway alterations in CR-1-expressing or shCR-1-expressing HCC cells and in the mouse hepatocytes induced by hepatocyte-specific overexpression of hCR-1 transgene. We found that AKT, Stat3 and JNK pathways were activated in CR-1-expressing BEL-7402 and HepG2 cells, as supported by the upregulation of p-AKT, p-GSK-3β, p-Stat3 and p-JNK (Fig. 5A), while AKT, Stat3 and JNK pathways were suppressed in shCR-1-expressing BEL-7402 and HepG2 cells, as supported by the down-regulation of p-AKT, p-GSK-3β, p-Stat3 and p-JNK (Fig. 5A). More importantly, we revealed that the AKT, Stat3, ERK and JNK pathways were significantly activated in the livers of RCLG/Alb-Cre transgenic mice, as supported by the notably elevated levels of p-AKT, p-GSK-3β, p-Stat3, p-ERK and p-JNK (Fig. 5B). We also found the increased expression of β-catenin in CR-1-expressing HCC cells (Fig. 5A) and the livers of RCLG/Alb-Cre mice (Fig. 5B), whereas the reduced expression of β-catenin was observed in shCR-1-expressing HCC cells (Fig. 5A). Moreover, qRT-PCR assay showed that the relative mRNA levels of IL-1, IL-6, Notch1 and TGF-β1 were significantly higher in the liver of RCLG/Alb-Cre mice than that of control mice (Fig. 5C). Taken together, CR-1 transgene overexpression in mouse liver and HCC cells significantly activates AKT, Stat3, ERK and JNK pathways, which is closely associated with hepatocyte proliferation, liver regeneration and hepatocelluar carcinogenesis.

10. Identification of HCC-related genes deregulated in RCLG/Alb-Cre transgenic livers by cDNA microarray

As there were no histological signs of precancerous lesions in liver samples from 3-, 6- or 8-month-old RCLG/Alb-Cre transgenic mice with many deregulated downstream pathways involved in HCC formation, malignant progression and poor prognosis, we next performed cDNA microarray analysis with RNA isolated from 4-month-old RCLG/Alb-Cre transgenic non-cancerous livers to represent the early or pre-cancerous phases of gene alterations. Data

analysis resulted in the identification of 211 differentially-expressed genes in non-cancerouss liver tissues from RCLG/Alb-Cre transgenic mice; among them, 48 genes were upregulated, and 163 genes were downregulated (Fig. S7 and Table S6). Among the 211 genes with remarkable expression changes, 113 deregulated genes (upregulated: 30; downregulated: 83) (Fig. 6A and Table S7) were closely associated with cellular proliferation, apoptosis, liver regeneration, stress responses, inflammation response, immune escape, defense response, acute-phase response, cellular malignant transformation, oncogenesis or cancer malignant progression and poor prognosis. We hypothesized that the genes that were deregulated in the 4-month-old liver tissues might reflect the direct effects of CR-1 expression.

To validate the microarray results, qRT-PCR was used to measure the expression of these selected genes in1-, 3- or 6-month-old livers of RCLG/Alb-Cre mice (Fig. 6B, C, D). The qRT-PCR results (Fig. 6B, C, D) confirmed the expression changes of 15 genes (i.e., Itih3, CD5L, G0S2, Klk1, Acaa1b, Ly6e, Foxred2, Rnase1, Pdk4, Srebf1, Dmbt1, Orm2, Tff1, Tff2 and Tff3) identified by microarray (Fig. 6A and Table S7). Although there were no histological signs of precancerous lesions in liver samples from 4-month-old RCLG/Alb-Cre transgenic mice, our aforementioned findings clearly indicate that gene expression and pathway dysregulation in the liver began in young RCLG/Alb-Cre mice.

Next, we further investigated the clinical roles of some genes selected from differentially expressed genes (DEGs) shown in Fig. 6A, B, C, D. Two GEO datasets revealed that the expression of Pdk4, G0S2, Plk2, Plk3 and Tff2 in HCC clinical specimens was significantly lower than their matched adjacent liver tissues (Fig. 7A, B), and the up-regulated expression of Srebf1 was observed in HCC tissues as compared with adjacent non-tumorous liver tissues (Fig. 7B), which is consistent with the expression changes of these genes in RCLG/Alb-Cre transgenic liver tissues (Fig. 6A, B, C,.D and Table S7). Furthermore, we selected some of the aforementioned genes dysregulated in RCLG/Alb-Cre transgenic livers (Fig. 6A, B, C, D and Table S7) to examine their expression profile in a cohort of human HCC clinical specimens by qRT-PCR. We found that the expressions of selected 6 genes (i.e., Pdk4, G0S2, Plk2, Plk3, Rnase1 and Klk1) were significantly reduced, and the expressions of selected 2 genes (i.e.,

Tmem176a and Tmem176b) were notably increased in HCC tissues when compared with matched non tumorous liver tissues (Fig. 7C, D), which is consistent with the expression changes of these genes in RCLG/Alb-Cre transgenic liver tissues (Fig. 6A, B, C, D and Table S7). Next, we performed tissue array analysis to compare Pdk4 protein levels between human HCC clinical specimens and adjacent non-tumorous liver tissues. Our data detected significantly lower levels of Pdk4 in HCC specimens than in control samples (Fig. 7E, F). Altogether, the observations that Pdk4 levels are reduced in both RCLG/Alb-Cre transgenic livers and HCC specimens and that loss of Pdk4 expression promotes proliferation, tumorigenicity, motility and invasion of HCC cells (our unpublished data) provide strong evidence that Pdk4 may function as a tumor suppressor in mice and in HCC.

Discussion

As described above, there has a FL-CR-1 mRNA transcript (2-kb) and a truncated 1.7-kb mRNA transcript from the human CR-1 gene[60, 61]. The results of the RT-PCR assay on RNA extracted from normal human tissues demonstrated that both the longer 2-kb and the shorter 1.7-kb CR-1 mRNA transcript forms were expressed in the cells of the lung, kidney, brain, testis, skeletal muscle, ovary and spleen, whereas the short CR-1 mRNA form was only present in several normal tissues such as the pancreas, heart, stomach, mammary gland, liver and placenta in humans[60]. This shorter mRNA is the only CR-1 transcript that is present in the majority of primary human colorectal carcinomas (7 out of 9 analyzed) and liver metastases from primary colon tumors (13 out of 14 analyzed)[60]. The results presented here illustrate for the first time that a truncated 1.7-kb mRNA transcript from the human CR-1 gene is dominantly expressed in adjacent non-tumorous liver tissues and primary HCC clinical tissue specimens (Fig. 1). Furthermore, the previous studies have illustrated that NT2/D1 cells and four different human embryonal carcinoma cell lines were found to only express FL-CR-1 mRNA transcript, but, in contrast, human colon carcinoma- and hepatocarcinoma-derived cell lines (i.e., SW480、SW620、LS174T、GEO、CBS、HepG2 and Hep3B) only expressed the truncated form of CR-1 mRNA[60, 61]. In this study, our RT-PCR analysis revealed that two CR-1 mRNA transcript forms from the human CR-1 gene

were expressed in QGY7701, HepG2, Hep3B, SNU-182 and SNU-387 cells, but the majority of CR-1 transcripts represent the SF-CR-1 in these aforementioned cells. Collectively, these data indicate that either FL-CR-1 mRNA transcript (2-kb) or SF-CR-1 mRNA transcript (1.7-kb) was expressed in different human normal and tumor tissues, and cancer cell lines, however, the majority of CR-1 transcripts represent the SF-CR-1 in these aforementioned human tumor tissues and cells.

In addition, Southern blot analysis illustrated that two different CR-1 mRNA transcripts that were present in NT2/D1, GEO and HepG2 cell lines were not due to alterations in the genomic DNA[60]. The previous study revealed a direct transcriptional regulation of SF-CR-1 mRNA transcript expression by the canonical Wnt/β-catenin/TCF signaling pathway through an intronic-exonic enhancer element, containing three tandem TCF/LEF binding sites within the CR-1 gene, in colon carcinoma and hepatoma cell lines (i.e., SW620 and HepG2 cells)[61], and that the SF-CR-1 mRNA is dominantly expressed in Wnt-active cell lines[61].

As described in the section of Introduction, CR-1 is a multifunctional modulator involved in embryogenesis, oncogenesis and cancer progression[20-27]. CR-1 is highly expressed in a variety of human cancers[21, 24, 32-37]. The truncated CR-1 mRNA lacks exon 1 and 2, but the putative open reading frame still maintains the EGF-like module, the cysteine-rich domain and the COOH-terminal linkage sequence[60, 61]. Although the biological functions of this truncated form of CR-1 that can be detected in human colon carcinomas and their hepatic metastases, and HCC clinical specimens have not yet been elucidated, the fact that the short form of CR-1 is a major transcript in such cancers[60, 61] suggests the importance of SF-CR-1 in cancer progression, which is required to be investigated in the future.

It is well known that embryonic genes such as Oct4[38-40] and CR-1[26, 41, 42] are not detected or expressed at low levels in normal adult tissues[20-27], whereas the re-expression of CR-1 was observed in numerous solid tumors[21, 24, 32-37]. The inappropriate activation of embryonic genes, such as Oct4[38-40] and CR-1[26, 41, 42], contributes to oncogenesis in somatic tissues. The overexpression of Cripto-1 transgene in

MMTV-CR-1 or WAP-CR-1 transgenic mouse mammary gland led to mammary epithelial hyperplasia and adenocarcinoma[26, 41], and the development of leiomyosarcoma of the uterus in MMTV-CR-1 transgenic mice[42]. As described above, the data from other labs[48-50] and this study clearly showed that CR-1 exerted its pro-tumorigenic influences on HCC progression. In this study, we observed that CR-1 transgenic overexpression in the liver of transgenic mice abnormally activated these aforementioned downstream pathways and led to the deregulated expression profile of genes, all of which are key regulators of cellular proliferation, inflammation response, cellular malignant transformation, hepatocelluar carcinogenesis or cancer malignant progression and poor prognosis, however, there were no histological signs of precancerous lesions, hepatocyte dysplasia and HCC formation in liver samples from 3-, 6- or 8-month-old RCLG/Alb-Cre transgenic mice, suggesting that the constitutive expression of CR-1 alone is not sufficient to promote hepatocarcinogenesis, unless other factors, i.e., a second hit, is present.

CR-1 exerts various cellular activities through activating its downstream pathways such as AKT, Wnt/β-catenin, Stat3, MAPK/ERK, TGF-β and Notch[23-26, 43, 48, 72, 73], all of which are involved in hepatocarcinogenesis or HCC malignant progression and poor prognosis[12, 13, 18, 19, 74-76]. The increased levels of β-catenin and phosphorylated AKT were detected in mammary gland tumor tissues from MMTV-CR-1 or WAP-CR-1 transgenic mice[26, 41] and in the leiomyosarcoma tissues of the uterus in MMTV-CR-1 transgenic mice[42]. In the present study, we also found that CR-1 transgene overexpression in RCLG/Alb-Cre transgenic mouse liver and HCC cells significantly activated AKT, Wnt/β-catenin, Stat3, MAPK/ERK, JNK, TGF-β and Notch pathways, all of which are closely associated with hepatocyte proliferation, liver regeneration or hepatocelluar carcinogenesis. Collectively, hepatocyte-specific overexpression of CR-1 transgene in transgenic mice can result in the abnormal activation of aforementioned signaling pathways involved in the premalignant alterations during hepatocarcinogenesis.

Among these identified 113 genes shown in Fig. 6A and Table S7, except for some genes with unknown functions, most of them encoded proteins related to cellular proliferation, cell cycle,

apoptosis, liver regeneration, DNA damage, stress responses, inflammation response, immune escape, defense response, acute-phase response, cellular malignant transformation, oncogenesis or cancer malignant progression and poor prognosis. These processes were previously reported to be involved mainly in various pathological injuries to the liver, or the development of HCC[77-80].

Among these identified genes, the upregulated genes (i.e., Orm2, Orm3, S100A8 and S100A9) and downregulated genes (i.e., DMBT1, Gsta2 and G0S2) in RCLG/Alb-Cre transgenic livers have been reported as important hepatocarcinogenic factors [81-85]. The transgenic mice with hepatocyte-specific overexpression of DNA binding protein A (dbpA) spontaneously developed liver tumors around 1.5 years old, but did not show any morphological changes in the liver around 30-40 weeks old[85]. Orm2 (Orosomucoid 2) and Orm3 (Orosomucoid 3), and G0S2 (G0/G1 switch gene 2) have been shown to be upregulated or downregulated in 31- and 32-week-old male dbpA transgenic mouse livers[85] and HCC tissues (Fig. 7), respectively. The downregulation of Gsta2 (glutathione-S-transferase, alpha type 2) mRNA was observed in the liver of the fenofibrate-treated rats, in which hepatocarcinogenesis was induced by fenofibrate[84]. Deleted in malignant brain tumours 1 (DMBT1)gene was downregulated in RCLG/Alb-Cre transgenic livers (Fig. 6 and Table S7) and HCC tissues[86], while the previous study showed that the down-expression of DMBT1 enhances the risk of malignant transformation of hepatic progenitor cells (HPCs)[81], suggesting that DMBT1 may play an important role in hepatocarcinogenesis. S100A8 and S100A9 exhibit pro-tumorigenic functions *in vitro* as both proteins promote tumor cell proliferation, migration and invasion of different tumor cell lines[87], while these observations have been validated also *in vivo* using mouse models, in which S100A8 and/or S100A9 induced tumor growth has been demonstrated for colon, brain, breast, thymus and thyroid cancers[82]. Notably, several lines of evidence indicate that S100A8 and/or S100A9 might be involved in HCC initiation and progress. The damage-associated molecular pattern molecules S100A8 and S100A9 are up-regulated in human liver cancer and correlates with poor differentiation[82, 83, 88]. The expression levels of the damage-associated molecular pattern molecules S100A8 and S100A9 were elevated in

serum and tissue samples from HCC patients[83, 88], whereas the expression of S100A9 but not S100A8 were also higher in blood serum and tissue samples from HBV-positive HCC patients than that in HBV-negative HCC patients [88]. In addition, S100A8/A9 promoted HCC cell survival, proliferation and invasion *in vitro* and these data were confirmed in a xenograft model, in which injection of recombinant S100A9 in subcutaneous tumors of transplanted HCC cells increased cancer size[82, 88]. A pro-tumorigenic function of S100A8/A9 in the carcinogen (DEN: diethylnitrosamine)-driven HCC model was observed, while S100A8/A9 ablation impaired liver cancer progression due to reduced cancer cell proliferation[82]. A synergistic function for S100A8 and S100A9 in HCC cells resulted in a significant induction of reactive oxygen species (ROS), accompanied by enhanced cell survival[82]. More importantly, S100A8 and S100A9 were identified as novel NF-μB target genes in HCC cells during inflammation-associated liver carcinogenesis[82]. These findings indicate that S100A8 and S100A9, forming a heterodimer called calprotectin, might be critically involved in HCC development. In this work, increased expression of S100A9 and S100A8in RCLG/Alb-Cre transgenic liver tissues might encourage hepatocyte cells to survive injury and ignored apoptotic signals, which would ultimately led to cell transformation.

The pyruvate dehydrogenase complex (PDC), a key regulator of tricarboxylic acid (TCA) cycle flux, catalyzes oxidative conversion of pyruvate into acetyl CoA and NADH in mitochondria, which is required for the TCA cycle and mitochondrial respiration, while phosphorylation of PDC is catalyzed in humans by any of four isozymes of the pyruvate dehydrogenase kinase (PDK1, PDK2, PDK3 and PDK4), which exhibit 70% homology[89-94]. Accumulating evidence has shown that PDK1-3 are closely associated with the metabolism of tumor cells because they can phosphorylate PDC, leading to the inactivation of PDC[89-94]. There is evidence showing that PDK4 acts as tumour suppressors because it is dramatically decreased in multiple human cancers, including breast, ovarian, colon and lung cancers[95-97], and HCC (this study). In this study, our results revealed the significantly decreased expression of PDK4 in RCLG/Alb-Cre transgenic livers (Fig. 6 and Table S7) and human HCC tissue samples (Fig. 7), and our unpublished data showed that PDK4 silencing by RNAi resulted in significantly enhanced proliferation, tumorigenicity, motility and invasion of HCC cells. Additionally, $PDK4^{-/-}$

livers showed increased hepatocyte proliferation, which was diminished by arsenic treatment[98]. Together, the aforementioned findings demonstrate that PDK4 may function as a tumor suppressor during hepatocarcinogenesisin mice and humans.

Previous works demonstrate that genes involved in the regulation of the cell cycle and apoptosis are frequently affected in HCC[78, 79, 99]. Unexpectedly, a relatively small number of genes (G0S2, Plk2, Plk3, Casp4, Casp8, S100A8 and S100A9) fell into these two groups in this work (Fig. 6A and Table S7). This may be explained by the use of relatively stringent criteria for selecting the candidate genes in the present study.

Some of these dysregulated genes observed in RCLG/Alb-Cre transgenic livers are known to exhibit the correspondingly altered expression in human HCC tissue samples and, in some cases, functionally contribute to hepatocarcinogenesis. Such genes include Tmem176a, Tmem176b, and , as well as other genes known to play a role in HCC such as C4b[100-102], Tsc22d3[103], Lgals4[104-106], Akr1c19[107], Vipr2[106, 108], Asns[109, 110], Cttn[111, 112], Nupr1[113-115], Prss3[116] and Dmbt1[81], and in animal liver cancer models such asSlpi[117], Akr1c19[107], Serpine2[118, 119] and Gdf15[120].

Although not directly reported in HCC pathogenesis, the deregulated expression of Ocel1[111], Ablim1[121], Tmed5[122-124], TMEM140[125], Sucnr1[126], Slc22a5[127-130], Efnb1[131-133], Zfhx1a[134, 135], Foxred2[136, 137], Reg3g[138, 139], Pdia2[140, 141], Rnase1[142-144], Pnliprp1[110, 145], Tmed6[146, 147] and Cuzd1[148, 149] has been shown to be closely related to other types of tumors.

The kallikrein-related peptidases (Klks) represent the largest family of secreted serine proteases within the human genome and are expressed in various tissues[150, 151]. Although they regulate several important physiological functions, Klks have also been implicated in numerous pathophysiological processes, including cancer[150, 151]. Interestingly, our transcriptional profiling also revealed significantly downregulated-expression changes of the family members of Klks in 4-month-old

RCLG/Alb-Cre transgenic livers, including Klk1, Klk15, Klk1b3, Klk1b4, Klk1b5, Klk1b8, Klk1b11, Klk1b21, Klk1b24, Klk1b26 and Klk1b27 (Fig. 6A, Table S7 and Table S8). Downregulation of Klk1 was validated by qRT-PCR in RCLG/Alb-Cre transgenic livers (Fig. 6) and HCC tissue samples (Fig. 7). Although not directly reported in HCC pathogenesis, the deregulated expression of human KLKs in many cancers has been shown to be closely related to the progression of other types of tumors[150, 151]. Additionally, a constantly increasing number of in vitro and in vivo studies demonstrate that these peptidases are now considered key players in the regulation of cancer cell growth, migration, invasion, chemo-resistance, and importantly, in mediating interactions between cancer cells and other cell populations found in the tumour microenvironment to facilitate cancer progression[150, 151]. However, the exact functions of these Klk genes during HCC progression and hepatocarcinogenesis need to be further investigated.

HCC is a major cause of cancer death, and its development is influenced by the status of oxidative stress, DNA damage and inflammation in the liver. Accumulating evidence has indicated that oxidative stress is associated with HCC development[152-154]. In this work, two genes encoding the antioxidant proteins glutathione S-transferase, alpha 1 (Gsta1) and glutathione S-transferase, alpha 2 (Gsta2) were identified to be down-regulated in RCLG/Alb-Cre transgenic livers, whereas a pro-oxidant inducer vanin 3 (Vnn3) was identified to be up-regulated in RCLG/Alb-Cre transgenic livers (Fig. 6 and Table S7). In RCLG/Alb-Cre transgenic livers, there are some of dysregulated genes involved in oxidative stress, including up-regulated gene [i.e., vanin 3 (Vnn3)] and down-regulated genes [i.e., glutathione S-transferase, alpha 1 (Gsta1) and glutathione S-transferase, alpha 2 (Gsta2)] (Fig. 6 and Table S7). Vanin/pantetheinase is highly expressed at gene and protein level in many organs, such as the liver, intestine and kidney, and many studies have elucidated the roles of vanin 1 (Vnn1), vanin 2 (Vnn2) and vanin 3 (Vnn3) as an oxidative stress inducer[155-158]. The previous study revealed the significant down-regulations of the oxidant defense genes (i.e., Gsta1 and Gsta2) in the liver of the fenofibrate-treated rats with fenofibrate-induced hepatocarcinogenesis[84]. Our finding indirectly reflects the existence of oxidative damage induced by CR-1 overexpression. In our work, increased expression of pro-oxidant inducer

Vnn3 and decreased expression of antioxidant genes (i.e., Gsta1 and Gsta2) in RCLG/Alb-Cre transgenic liver tissues might aid the oxidatively damaged hepatocytes to escape from apoptosis, possibly induced by increased reactive oxygen species (ROS), and to favor the onset of hepatocarcinogenesis.

Increased evidence has shown that DNA damage is involved in hepatocarcinogenesis[159, 160]. In our work, we revealed the significantly down-regulated expression of polo-like kinase 2 (Plk2) and polo-like kinase 3 (Plk3) involved in DNA damage in RCLG/Alb-Cre transgenic livers (Fig. 6 and Table S7) and human HCC tissue samples (Fig. 7). There is evidence showing that Plk2 and Plk3 act as tumour suppressors through their functions in the p53 signaling network, which guards the cell against various stress signals[161-165]. Emerging evidence suggests an antiproliferative impact of Plk2 and Plk3 during mitosis[161-165]. Plk3 links DNA damage to cell cycle arrest through the ATM/p53 pathway, and Plk3-deficient mice develop tumours[161-165]. Furthermore, Plk2 and Plk3 are involved in checkpoint-mediated cell cycle arrest to ensure genetic stability, thereby inhibiting the accumulation of genetic defects[161-165]. In this study, the decreased expression of Plk2 and Plk3 in RCLG/Alb-Cre transgenic liver tissues might result in genetic mutations in the oxidatively damaged hepatocytes and expansion of initiated cells, eventually contributing to the onset of liver carcinogenesis.

HCC is an inflammation-induced cancer[153, 166-169]. It is known that chronic liver inflammation leads to oxidative/nitrosative stress and lipid peroxidation, generating excess oxidative stress, together with aldehydes which can react with DNA bases to form promutagenic DNA adducts [153, 166-169]. In this work, there are many of up-regulated genes involved in liver inflammation (i.e., CD5L, S100A8, S100A9, Timd4 and Rgs16), immune escape (i.e.,Orm2, Orm3, IGHG1, IGHG2B, IGHG2C and IGKV16-104), acute-phase response (i.e., Orm2,Orm3, Saa1, Saa3, Itih3 and Itih4) and defense response (i.e., Ly6e) (Fig. 6 and Table S7) in RCLG/Alb-Cre transgenic livers.

Api6/AIM/Spa/CD5L was upregulated in HCC and promoted liver cancer cell proliferation and antiapoptotic responses by binding to HSPA5 (GRP78)[170]. CD5L is a pleiotropic player in liver fibrosis controlling damage, fibrosis and immune cell content[171]. CD5L transgenic overexpression in the alveolar type II epithelial cells (AT II cells) of transgenic mice induced malignant transformation and spontaneous lung adenocarcinoma by limiting lung epithelial cell apoptosis and promoting immune escape[172]. Moreover, CD5L overexpression in AT II cells increased the concentrations of proinflammatory cytokines/chemokines in bronchoalveolar lavage fluid and serum, promoting expansion of myeloid-derived suppressor cells (MDSC) in lung and blood, while lung MDSCs suppressed T-cell proliferation and activity *in vitro* and reduced levels of T cells *in vivo* following doxycycline treatment to activate CD5L transgene[172]. The presence of IGHG1 in pancreatic cancer cells constituted an important element responsible for tumor cell proliferation and immune evasion mechanisms[173].

Tumor immunoevasion is an advanced phase of cancer immunosurveillance in which tumor cells acquire the ability to circumvent host immune systems and exploit protumorigenic inflammation[174]. T-cell immunoglobulin mucin (TIM) gene family members have emerged as critical checkpoint proteins that regulate multiple immune response phases and maintain immune homeostasis[174]. Accumulating evidence demonstrates that tumor cells exploit TIM gene family members to evade immunosurveillance, whereas TIM gene family members facilitate the prevention of inflammation-related tumor progression[174]. Timd4 (T-cell immunoglobulin domain and mucin domain 4; also known as TIM4) is known to play critical roles in the regulation of tumor immunosurveillance and anti-tumor immunity[174]. Timd4 in non-small-cell lung cancer (NSCLC) tissues was significantly higher than that of the adjacent tissues, and Timd4 overexpression promoted lung cancer cell growth and proliferation[175]. NF-μB signaling pathway has been recently shown to participate in inflammation-induced cancer progression, and S100A8 and S100A9 were identified as novel NF-μB target genes in HCC cells during inflammation-associated liver carcinogenesis[82].

The complex series of reactions initiated in response to infection, physical trauma, or malignancy is called the acute-phase response (APR). As acute-phase proteins, Orm2 and

Orm3 play important roles in anti-inflammation and immunomodulation[176]. Orm2 is frequently downregulated in HCC tissues and is negatively associated with tumor progression and intrahepatic metastasis[176]. The serum concentration of ITIH4, a member of the acute-phase protein family, increased during acute-phase processes in human patients, and ITIH4 is up-regulated by interleukin-6 in hepatocarcinoma HepG2 cells[177]. Collectively, this gene signature was enriched for the inflammatory and host immunity processes; both crucially involved in HCC development.

Conclusion

In conclusion, we provided the first evidence that HCC clinical tissue specimens dominantly expressed the short form CR-1 mRNA, but the biological effects of this truncated form of CR-1 in HCC progression remains to be investigated in the future. Hepatocyte-specific overexpression of CR-1 in transgenic mice abnormally activated these aforementioned downstream pathways and led to the deregulated expression profile of genes, all of which are key regulators of cellular proliferation, inflammation response, cellular malignant transformation, oncogenesis or cancer malignant progression and poor prognosis, however, these abnormally molecular alterations induced by the enforced CR-1 transgene expression in mouse liver is not sufficient to initiate hepatocarcinogenesis in mice.

Declarations

Data for reference

RNA sequencing data were submitted to GEO database with accession number GSE64255.

Authors' contributions

DX, LXL and KX conceived and designed the study; LXL, YL, YQL, JSJ, WTZ, FW, SHH, YCW, YLL and XYL performed the experiments; DX, LXL, KX, YL, YQL, JSJ and WTZ analyzed the data; GQD and LXH contributed essential reagents or tools; DX and LXL wrote the paper. All authors read and approved the final manuscript.

Acknowledgements

We thank Prof. Peter C. Gray (The Salk Institute for Biological Studies, USA.), Prof. David S. Salomon (Center for Cancer Research, National Cancer Institute, USA) and Prof. Manuela Martins-Green (University of California, USA) for generously providing plasmids.

Competing interest

The authors who have taken part in this study declare that they do not have anything to disclose regarding conflicts of interest concerning this manuscript.

Availability of data and materials

The datasets used and/or analyzed during the current study are available from the corresponding author on reasonable request.

Consent for publication

Not applicable.

Ethics approval and consent to participate

All animal protocols were approved by the Institutional Animal Care and Use Committee (IACUC) at the Institute of Laboratory Animal Center, Southern Medical University (L2017068).

Funding sources

This work was supported by the National Natural Science Foundation of China (Grant No. 81872209, 81672689, 81372896 and 81172587, to D. Xiao; Grant No. 81600488 and 81870602, to X.-L. Lin; Grant No. 81702778, to J.S. Jia), the Natural Science Foundation of Guangdong Province of China (Grant No. 2014A030313294 to D. Xiao), the Science and Technology Planning Project of Guangdong Province of China (Grant No. 2009B060300008, 2013B060300013 and 2017A010105017, to D. Xiao; Grant No. 2017A030303018, to J.S. Jia; Grant No. 2015A030302024, to X.-L. Lin), the China Postdoctoral Science Foundation(Grant No. 2015M572338, 2016T90792, 2017M622740 and 2018T110884, to X.-L. Lin) and the Medical Scientific Research Foundation of Guangdong Province of China (Grant No.A2017420, to J.S. Jia).

References

1. Akinyemiju, T., et al., *The Burden of Primary Liver Cancer and Underlying Etiologies From 1990 to 2015 at the Global, Regional, and National Level Results From the Global Burden of Disease Study 2015.* Jama Oncology, 2017. **3**(12): p. 1683-1691.
2. Erridge, S., et al., *Meta-analysis of determinants of survival following treatment of recurrent hepatocellular carcinoma.* Br J Surg, 2017. **104**(11): p. 1433-1442.
3. Zhao, W.T., et al., *miR-26a promotes hepatocellular carcinoma invasion and metastasis by inhibiting PTEN and inhibits cell growth by repressing EZH2.* Lab Invest, 2019. **99**(10): p. 1484-1500.
4. Anstee, Q.M., et al., *From NASH to HCC: current concepts and future challenges.* Nat Rev Gastroenterol Hepatol, 2019. **16**(7): p. 411-428.
5. Arzumanyan, A., H.M. Reis, and M.A. Feitelson, *Pathogenic mechanisms in HBV- and HCV-associated hepatocellular carcinoma.* Nat Rev Cancer, 2013. **13**(2): p. 123-35.
6. Calderaro, J., et al., *Molecular and histological correlations in liver cancer.* Journal of Hepatology, 2019. **71**(3): p. 616-630.
7. Erkekoglu, P., et al., *Hepatocellular Carcinoma and Possible Chemical and Biological Causes: A Review.* J Environ Pathol Toxicol Oncol, 2017. **36**(2): p. 171-190.
8. Farazi, P.A. and R.A. DePinho, *Hepatocellular carcinoma pathogenesis: from genes to environment.* Nat Rev Cancer, 2006. **6**(9): p. 674-87.
9. Hlady, R.A. and K.D. Robertson, *Genetic and Epigenetic Heterogeneity in Normal Liver Homeostasis and Its Implications for Liver Disease and Hepatocellular Cancer.* Semin Liver Dis, 2018. **38**(1): p. 41-50.
10. Singh, A.K., R. Kumar, and A.K. Pandey, *Hepatocellular Carcinoma: Causes, Mechanism of Progression and Biomarkers.* Curr Chem Genom Transl Med, 2018. **12**: p. 9-26.
11. Yang, J.D., et al., *A global view of hepatocellular carcinoma: trends, risk, prevention and management.* Nat Rev Gastroenterol Hepatol, 2019. **16**(10): p. 589-604.
12. Colnot, S., et al., *Liver-targeted disruption of Apc in mice activates beta-catenin signaling and leads to hepatocellular carcinomas.* Proc Natl Acad Sci U S A, 2004. **101**(49): p. 17216-21.
13. Morris, S.M., et al., *Transforming growth factor-beta signaling promotes hepatocarcinogenesis induced by p53 loss.* Hepatology, 2012. **55**(1): p. 121-31.
14. Ozturk, M., *Genetic aspects of hepatocellular carcinogenesis.* Semin Liver Dis, 1999. **19**(3): p. 235-42.
15. Sonntag, R., et al., *Cyclin E1 and cyclin-dependent kinase 2 are critical for initiation, but not for progression of hepatocellular carcinoma.* Proc Natl Acad Sci U S A, 2018. **115**(37): p. 9282-9287.
16. Terradillos, O., et al., *The hepatitis B virus X gene potentiates c-myc-induced liver oncogenesis in transgenic mice.* Oncogene, 1997. **14**(4): p. 395-404.
17. Tomas-Loba, A., et al., *p38gamma is essential for cell cycle progression and liver tumorigenesis.* Nature, 2019. **568**(7753): p. 557-560.
18. Wang, W., et al., *Wnt/beta-Catenin Signaling in Liver Cancers.* Cancers (Basel), 2019. **11**(7).
19. Ye, H., et al., *Synergistic function of Kras mutation and HBx in initiation and progression of hepatocellular carcinoma in mice.* Oncogene, 2014. **33**(43): p. 5133-8.
20. Bianco, C., et al., *Role of Cripto-1 in stem cell maintenance and malignant progression.* Am J Pathol, 2010. **177**(2): p. 532-40.
21. de Castro, N.P., et al., *Cripto-1: an embryonic gene that promotes tumorigenesis.* Future Oncol, 2010. **6**(7): p. 1127-42.
22. Kalyan, A., et al., *Nodal Signaling as a Developmental Therapeutics Target in Oncology.* Mol Cancer Ther, 2017. **16**(5): p. 787-792.

23. Klauzinska, M., et al., *The multifaceted role of the embryonic gene Cripto-1 in cancer, stem cells and epithelial-mesenchymal transition.* Semin Cancer Biol, 2014. **29**: p. 51-8.
24. Rangel, M.C., et al., *Role of Cripto-1 during epithelial-to-mesenchymal transition in development and cancer.* Am J Pathol, 2012. **180**(6): p. 2188-200.
25. Nagaoka, T., et al., *An evolving web of signaling networks regulated by Cripto-1.* Growth Factors, 2012. **30**(1): p. 13-21.
26. Strizzi, L., et al., *Cripto-1: a multifunctional modulator during embryogenesis and oncogenesis.* Oncogene, 2005. **24**(37): p. 5731-41.
27. Lin, X., et al., *Ectopic expression of Cripto-1 in transgenic mouse embryos causes hemorrhages, fatal cardiac defects and embryonic lethality.* Sci Rep, 2016. **6**: p. 34501.
28. Chu, J., et al., *Non-cell-autonomous role for Cripto in axial midline formation during vertebrate embryogenesis.* Development, 2005. **132**(24): p. 5539-51.
29. Ding, J., et al., *Cripto is required for correct orientation of the anterior-posterior axis in the mouse embryo.* Nature, 1998. **395**(6703): p. 702-7.
30. Dono, R., et al., *The murine cripto gene: expression during mesoderm induction and early heart morphogenesis.* Development, 1993. **118**(4): p. 1157-68.
31. Xu, C., et al., *Abrogation of the Cripto gene in mouse leads to failure of postgastrulation morphogenesis and lack of differentiation of cardiomyocytes.* Development, 1999. **126**(3): p. 483-94.
32. Ciardiello, F., et al., *Differential expression of epidermal growth factor-related proteins in human colorectal tumors.* Proc Natl Acad Sci U S A, 1991. **88**(17): p. 7792-6.
33. Gong, Y.P., et al., *Overexpression of Cripto and its prognostic significance in breast cancer: a study with long-term survival.* Eur J Surg Oncol, 2007. **33**(4): p. 438-43.
34. Saeki, T., et al., *Differential immunohistochemical detection of amphiregulin and cripto in human normal colon and colorectal tumors.* Cancer Res, 1992. **52**(12): p. 3467-73.
35. Wu, Z., et al., *Cripto-1 overexpression is involved in the tumorigenesis of nasopharyngeal carcinoma.* BMC Cancer, 2009. **9**: p. 315.
36. Zhong, X.Y., et al., *Positive association of up-regulated Cripto-1 and down-regulated E-cadherin with tumour progression and poor prognosis in gastric cancer.* Histopathology, 2008. **52**(5): p. 560-8.
37. Xu, C.H., et al., *Elevated expression of Cripto-1 correlates with poor prognosis in non-small cell lung cancer.* Tumour Biol, 2014. **35**(9): p. 8673-8.
38. Beachy, P.A., S.S. Karhadkar, and D.M. Berman, *Tissue repair and stem cell renewal in carcinogenesis.* Nature, 2004. **432**(7015): p. 324-31.
39. Gidekel, S., et al., *Oct-3/4 is a dose-dependent oncogenic fate determinant.* Cancer Cell, 2003. **4**(5): p. 361-70.
40. Hochedlinger, K., et al., *Ectopic expression of Oct-4 blocks progenitor-cell differentiation and causes dysplasia in epithelial tissues.* Cell, 2005. **121**(3): p. 465-77.
41. Sun, Y., et al., *Overexpression of human Cripto-1 in transgenic mice delays mammary gland development and differentiation and induces mammary tumorigenesis.* Am J Pathol, 2005. **167**(2): p. 585-97.
42. Strizzi, L., et al., *Development of leiomyosarcoma of the uterus in MMTV-CR-1 transgenic mice.* J Pathol, 2007. **211**(1): p. 36-44.
43. Francescangeli, F., et al., *Dynamic regulation of the cancer stem cell compartment by Cripto-1 in colorectal cancer.* Cell Death Differ, 2015. **22**(10): p. 1700-13.
44. Castro, N.P., et al., *Cripto-1 as a novel therapeutic target for triple negative breast cancer.* Oncotarget, 2015. **6**(14): p. 11910-29.
45. Strizzi, L., et al., *The significance of a Cripto-1 positive subpopulation of human melanoma cells exhibiting stem*

cell-like characteristics. Cell Cycle, 2013. **12**(9): p. 1450-6.

46. Liu, Q., et al., *Cripto-1 acts as a functional marker of cancer stem-like cells and predicts prognosis of the patients in esophageal squamous cell carcinoma.* Mol Cancer, 2017. **16**(1): p. 81.
47. Ebert, A.D., et al., *Cripto-1-induced increase in vimentin expression is associated with enhanced migration of human Caski cervical carcinoma cells.* Exp Cell Res, 2000. **257**(1): p. 223-9.
48. Lo, R.C., et al., *Cripto-1 contributes to stemness in hepatocellular carcinoma by stabilizing Dishevelled-3 and activating Wnt/beta-catenin pathway.* Cell Death Differ, 2018. **25**(8): p. 1426-1441.
49. Wang, J.H., et al., *Elevated expression of Cripto-1 correlates with poor prognosis in hepatocellular carcinoma.* Oncotarget, 2015. **6**(33): p. 35116-28.
50. Zhang, Y., et al., *High level of serum Cripto-1 in hepatocellular carcinoma, especially with hepatitis B virus infection.* Medicine (Baltimore), 2018. **97**(35): p. e11781.
51. Li, X., et al., *Klf4 reduces stemness phenotype, triggers mesenchymal-epithelial transition (MET)-like molecular changes, and prevents tumor progression in nasopharygeal carcinoma.* Oncotarget, 2017. **8**(55): p. 93924-93941.
52. Lin, X., et al., *Overexpression of miR-155 in the liver of transgenic mice alters the expression profiling of hepatic genes associated with lipid metabolism.* PLoS One, 2015. **10**(3): p. e0118417.
53. Lin, X., et al., *miR-155 accelerates proliferation of mouse hepatocytes during liver regeneration by directly targeting SOCS1.* Am J Physiol Gastrointest Liver Physiol, 2018. **315**(4): p. G443-G453.
54. Liu, Y.M., et al., *Abnormalities of hair structure and skin histology derived from CRISPR/Cas9-based knockout of phospholipase C-delta 1 in mice.* J Transl Med, 2018. **16**(1): p. 141.
55. Rong, X.X., et al., *Recognition and killing of cancer stem-like cell population in hepatocellular carcinoma cells by cytokine-induced killer cells via NKG2d-ligands recognition.* Oncoimmunology, 2016. **5**(3): p. e1086060.
56. Shi, J.W., et al., *Direct conversion of pig fibroblasts to chondrocyte-like cells by c-Myc.* Cell Death Discov, 2019. **5**: p. 55.
57. Sun, Y., et al., *Phenotypic changes of human cells in human-rat liver during partial hepatectomy-induced regeneration.* World J Gastroenterol, 2009. **15**(29): p. 3611-20.
58. Wang, S.C., et al., *Hes1 triggers epithelial-mesenchymal transition (EMT)-like cellular marker alterations and promotes invasion and metastasis of nasopharyngeal carcinoma by activating the PTEN/AKT pathway.* Oncotarget, 2015. **6**(34): p. 36713-30.
59. Xie, R., et al., *Targeted Disruption of miR-17-92 Impairs Mouse Spermatogenesis by Activating mTOR Signaling Pathway.* Medicine (Baltimore), 2016. **95**(7): p. e2713.
60. Baldassarre, G., et al., *A truncated form of teratocarcinoma-derived growth factor-1 (cripto-1) mRNA expressed in human colon carcinoma cell lines and tumors.* Tumour Biol, 2001. **22**(5): p. 286-93.
61. Hamada, S., et al., *beta-Catenin/TCF/LEF regulate expression of the short form human Cripto-1.* Biochem Biophys Res Commun, 2007. **355**(1): p. 240-4.
62. Gray, P.C., et al., *Cripto binds transforming growth factor beta (TGF-beta) and inhibits TGF-beta signaling.* Mol Cell Biol, 2006. **26**(24): p. 9268-78.
63. Shi, J.W., et al., *The enforced expression of c-Myc in pig fibroblasts triggers mesenchymal-epithelial transition (MET) via F-actin reorganization and RhoA/Rock pathway inactivation.* Cell Cycle, 2013. **12**(7): p. 1119-27.
64. Watanabe, K., et al., *Requirement of glycosylphosphatidylinositol anchor of Cripto-1 for trans activity as a Nodal co-receptor.* J Biol Chem, 2007. **282**(49): p. 35772-86.
65. Zheng, L., C.N. Njauw, and M. Martins-Green, *A hCXCR1 transgenic mouse model containing a conditional color-switching system for imaging of hCXCL8/IL-8 functions in vivo.* J Leukoc Biol, 2007. **82**(5): p. 1247-56.
66. Zheng, L., C.N. Njauw, and M. Martins-Green, *A one-plasmid conditional color-switching transgenic system for*

multimodal bioimaging. Transgenic Res, 2008. **17**(4): p. 741-7.

67. Nagy, A., Gertsenstein, M., Vintersten, K. & Behringer, R, *Manipulating the mouse embryo : a laboratory manual*. 2003: Cold Spring Harbor Laboratory Press.
68. Lin, X., et al., *Simple and rapid determination of homozygous transgenic mice via in vivo fluorescence imaging.* Oncotarget, 2015. **6**(36): p. 39073-87.
69. Wei, F., et al., *Cytokine-induced killer cells efficiently kill stem-like cancer cells of nasopharyngeal carcinoma via the NKG2D-ligands recognition.* Oncotarget, 2015. **6**(33): p. 35023-39.
70. Jia, J., et al., *R/L, a double reporter mouse line that expresses luciferase gene upon Cre-mediated excision, followed by inactivation of mRFP expression.* Genome, 2016. **59**(10): p. 816-826.
71. Postic, C., et al., *Dual roles for glucokinase in glucose homeostasis as determined by liver and pancreatic beta cell-specific gene knock-outs using Cre recombinase.* J Biol Chem, 1999. **274**(1): p. 305-15.
72. Kannan, S., et al., *Cripto enhances the tyrosine phosphorylation of Shc and activates mitogen-activated protein kinase (MAPK) in mammary epithelial cells.* J Biol Chem, 1997. **272**(6): p. 3330-5.
73. Zhang, J.G., J. Zhao, and Y. Xin, *Significance and relationship between Cripto-1 and p-STAT3 expression in gastric cancer and precancerous lesions.* World J Gastroenterol, 2010. **16**(5): p. 571-7.
74. Schmitz, K.J., et al., *Activation of the ERK and AKT signalling pathway predicts poor prognosis in hepatocellular carcinoma and ERK activation in cancer tissue is associated with hepatitis C virus infection.* J Hepatol, 2008. **48**(1): p. 83-90.
75. Wang, S.N., et al., *Phosphorylated p38 and JNK MAPK proteins in hepatocellular carcinoma.* Eur J Clin Invest, 2012. **42**(12): p. 1295-301.
76. Yang, S.F., et al., *Altered p-STAT3 (tyr705) expression is associated with histological grading and intratumour microvessel density in hepatocellular carcinoma.* J Clin Pathol, 2007. **60**(6): p. 642-8.
77. Hajjou, M., et al., *cDNA microarray analysis of HBV transgenic mouse liver identifies genes in lipid biosynthetic and growth control pathways affected by HBV.* J Med Virol, 2005. **77**(1): p. 57-65.
78. Patil, M.A., et al., *An integrated data analysis approach to characterize genes highly expressed in hepatocellular carcinoma.* Oncogene, 2005. **24**(23): p. 3737-47.
79. Segal, E., et al., *From signatures to models: understanding cancer using microarrays.* Nat Genet, 2005. **37 Suppl**: p. S38-45.
80. Okabe, H., et al., *Genome-wide analysis of gene expression in human hepatocellular carcinomas using cDNA microarray: identification of genes involved in viral carcinogenesis and tumor progression.* Cancer Res, 2001. **61**(5): p. 2129-37.
81. Deng, H., et al., *Expression of deleted in malignant brain tumours 1 (DMBT1) relates to the proliferation and malignant transformation of hepatic progenitor cells in hepatitis B virus-related liver diseases.* Histopathology, 2012. **60**(2): p. 249-60.
82. De Ponti, A., et al., *A pro-tumorigenic function of S100A8/A9 in carcinogen-induced hepatocellular carcinoma.* Cancer Lett, 2015. **369**(2): p. 396-404.
83. Nemeth, J., et al., *S100A8 and S100A9 are novel nuclear factor kappa B target genes during malignant progression of murine and human liver carcinogenesis.* Hepatology, 2009. **50**(4): p. 1251-62.
84. Nishimura, J., et al., *Possible involvement of oxidative stress in fenofibrate-induced hepatocarcinogenesis in rats.* Arch Toxicol, 2008. **82**(9): p. 641-54.
85. Tobita, H., et al., *Gene expression profile of DNA binding protein A transgenic mice.* Int J Oncol, 2006. **29**(3): p. 673-9.
86. Frau, M., et al., *An expression signature of phenotypic resistance to hepatocellular carcinoma identified by cross-species gene expression analysis.* Cell Oncol (Dordr), 2012. **35**(3): p. 163-73.

87. Markowitz, J. and W.E. Carson, 3rd, *Review of S100A9 biology and its role in cancer.* Biochim Biophys Acta, 2013. **1835**(1): p. 100-9.
88. Duan, L., et al., *HBx-induced S100A9 in NF-kappaB dependent manner promotes growth and metastasis of hepatocellular carcinoma cells.* Cell Death Dis, 2018. **9**(6): p. 629.
89. Jeoung, N.H., *Pyruvate Dehydrogenase Kinases: Therapeutic Targets for Diabetes and Cancers.* Diabetes Metab J, 2015. **39**(3): p. 188-97.
90. Zhang, S.L., et al., *Development of pyruvate dehydrogenase kinase inhibitors in medicinal chemistry with particular emphasis as anticancer agents.* Drug Discov Today, 2015. **20**(9): p. 1112-9.
91. Saunier, E., C. Benelli, and S. Bortoli, *The pyruvate dehydrogenase complex in cancer: An old metabolic gatekeeper regulated by new pathways and pharmacological agents.* Int J Cancer, 2016. **138**(4): p. 809-17.
92. Stacpoole, P.W., *Therapeutic Targeting of the Pyruvate Dehydrogenase Complex/Pyruvate Dehydrogenase Kinase (PDC/PDK) Axis in Cancer.* J Natl Cancer Inst, 2017. **109**(11).
93. Sugden, M.C. and M.J. Holness, *Recent advances in mechanisms regulating glucose oxidation at the level of the pyruvate dehydrogenase complex by PDKs.* Am J Physiol Endocrinol Metab, 2003. **284**(5): p. E855-62.
94. Zhao, L., et al., *miR-504 mediated down-regulation of nuclear respiratory factor 1 leads to radio-resistance in nasopharyngeal carcinoma.* Oncotarget, 2015. **6**(18): p. 15995-6018.
95. Blouin, J.M., et al., *Butyrate elicits a metabolic switch in human colon cancer cells by targeting the pyruvate dehydrogenase complex.* Int J Cancer, 2011. **128**(11): p. 2591-601.
96. Grassian, A.R., et al., *Erk regulation of pyruvate dehydrogenase flux through PDK4 modulates cell proliferation.* Genes Dev, 2011. **25**(16): p. 1716-33.
97. Sun, Y., et al., *Metabolic and transcriptional profiling reveals pyruvate dehydrogenase kinase 4 as a mediator of epithelial-mesenchymal transition and drug resistance in tumor cells.* Cancer Metab, 2014. **2**(1): p. 20.
98. Choiniere, J., J. Wu, and L. Wang, *Pyruvate Dehydrogenase Kinase 4 Deficiency Results in Expedited Cellular Proliferation through E2F1-Mediated Increase of Cyclins.* Mol Pharmacol, 2017. **91**(3): p. 189-196.
99. Ng, R.K., et al., *cDNA microarray analysis of early gene expression profiles associated with hepatitis B virus X protein-mediated hepatocarcinogenesis.* Biochem Biophys Res Commun, 2004. **322**(3): p. 827-35.
100. Dalal, K., et al., *Differentially expressed serum host proteins in hepatitis B and C viral infections.* Virusdisease, 2018. **29**(4): p. 468-477.
101. Ehsani Ardakani, M.J., et al., *Evaluation of liver cirrhosis and hepatocellular carcinoma using Protein-Protein Interaction Networks.* Gastroenterol Hepatol Bed Bench, 2016. **9**(Suppl1): p. S14-S22.
102. Feng, G., et al., *Hepatitis B virus X protein up-regulates C4b-binding protein alpha through activating transcription factor Sp1 in protection of hepatoma cells from complement attack.* Oncotarget, 2016. **7**(19): p. 28013-26.
103. Takagi, K., et al., *High TSC22D3 and low GBP1 expression in the liver is a risk factor for early recurrence of hepatocellular carcinoma.* Exp Ther Med, 2011. **2**(3): p. 425-431.
104. Bacigalupo, M.L., et al., *Hierarchical and selective roles of galectins in hepatocarcinogenesis, liver fibrosis and inflammation of hepatocellular carcinoma.* World J Gastroenterol, 2013. **19**(47): p. 8831-49.
105. Cai, Z., et al., *Galectin-4 serves as a prognostic biomarker for the early recurrence / metastasis of hepatocellular carcinoma.* Cancer Sci, 2014. **105**(11): p. 1510-7.
106. Kondoh, N., et al., *Identification and characterization of genes associated with human hepatocellular carcinogenesis.* Cancer Res, 1999. **59**(19): p. 4990-6.
107. Torres-Mena, J.E., et al., *Aldo-Keto Reductases as Early Biomarkers of Hepatocellular Carcinoma: A Comparison Between Animal Models and Human HCC.* Dig Dis Sci, 2018. **63**(4): p. 934-944.
108. Hara, M., et al., *Vasoactive intestinal peptide increases apoptosis of hepatocellular carcinoma by inhibiting the*

cAMP/Bcl-xL pathway. Cancer Sci, 2019. **110**(1): p. 235-244.

109. Li, W. and C. Dong, *Polymorphism in asparagine synthetase is associated with overall survival of hepatocellular carcinoma patients.* BMC Gastroenterol, 2017. **17**(1): p. 79.
110. Zhang, B., et al., *Asparagine synthetase is an independent predictor of surgical survival and a potential therapeutic target in hepatocellular carcinoma.* Br J Cancer, 2013. **109**(1): p. 14-23.
111. Li, Y., et al., *The HBx-CTTN interaction promotes cell proliferation and migration of hepatocellular carcinoma via CREB1.* Cell Death Dis, 2019. **10**(6): p. 405.
112. Chuma, M., et al., *Overexpression of cortactin is involved in motility and metastasis of hepatocellular carcinoma.* J Hepatol, 2004. **41**(4): p. 629-36.
113. Chen, C.Y., et al., *Induction of nuclear protein-1 by thyroid hormone enhances platelet-derived growth factor A mediated angiogenesis in liver cancer.* Theranostics, 2019. **9**(8): p. 2361-2379.
114. Emma, M.R., et al., *NUPR1, a new target in liver cancer: implication in controlling cell growth, migration, invasion and sorafenib resistance.* Cell Death Dis, 2016. **7**(6): p. e2269.
115. Bak, Y., et al., *Hepatitis B virus X promotes hepatocellular carcinoma development via nuclear protein 1 pathway.* Biochem Biophys Res Commun, 2015. **466**(4): p. 676-81.
116. Lin, B., et al., *Epigenetic silencing of PRSS3 provides growth and metastasis advantage for human hepatocellular carcinoma.* J Mol Med (Berl), 2017. **95**(11): p. 1237-1249.
117. Matsushita, J., et al., *The DNA methylation profile of liver tumors in C3H mice and identification of differentially methylated regions involved in the regulation of tumorigenic genes.* BMC Cancer, 2018. **18**(1): p. 317.
118. Chen, L., et al., *Enhancement of DEN-induced liver tumourigenesis in hepatocyte-specific Lass2-knockout mice coincident with upregulation of the TGF-beta1-Smad4-PAI-1 axis.* Oncol Rep, 2014. **31**(2): p. 885-93.
119. Majumder, S., et al., *Loss of metallothionein predisposes mice to diethylnitrosamine-induced hepatocarcinogenesis by activating NF-kappaB target genes.* Cancer Res, 2010. **70**(24): p. 10265-76.
120. Zimmers, T.A., et al., *Effect of in vivo loss of GDF-15 on hepatocellular carcinogenesis.* J Cancer Res Clin Oncol, 2008. **134**(7): p. 753-9.
121. Kwong, L.N. and L. Chin, *Chromosome 10, frequently lost in human melanoma, encodes multiple tumor-suppressive functions.* Cancer Res, 2014. **74**(6): p. 1814-21.
122. Boyd, K.D., et al., *Mapping of chromosome 1p deletions in myeloma identifies FAM46C at 1p12 and CDKN2C at 1p32.3 as being genes in regions associated with adverse survival.* Clin Cancer Res, 2011. **17**(24): p. 7776-84.
123. Scaravilli, M., et al., *Mapping of the chromosomal amplification 1p21-22 in bladder cancer.* BMC Res Notes, 2014. **7**: p. 547.
124. Yang, Z., et al., *GRSF1-mediated MIR-G-1 promotes malignant behavior and nuclear autophagy by directly upregulating TMED5 and LMNB1 in cervical cancer cells.* Autophagy, 2019. **15**(4): p. 668-685.
125. Li, B., et al., *TMEM140 is associated with the prognosis of glioma by promoting cell viability and invasion.* J Hematol Oncol, 2015. **8**: p. 89.
126. Gao, Y., et al., *Superparamagnetic iron oxide nanoparticle-mediated expression of miR-326 inhibits human endometrial carcinoma stem cell growth.* Int J Nanomedicine, 2019. **14**: p. 2719-2731.
127. Zou, D., et al., *Integrative expression quantitative trait locus-based analysis of colorectal cancer identified a functional polymorphism regulating SLC22A5 expression.* Eur J Cancer, 2018. **93**: p. 1-9.
128. Jaruskova, M., et al., *Genotypes of SLC22A4 and SLC22A5 regulatory loci are predictive of the response of chronic myeloid leukemia patients to imatinib treatment.* J Exp Clin Cancer Res, 2017. **36**(1): p. 55.
129. Wang, C., et al., *SLC22A5/OCTN2 expression in breast cancer is induced by estrogen via a novel intronic estrogen-response element (ERE).* Breast Cancer Res Treat, 2012. **134**(1): p. 101-15.
130. Scalise, M., et al., *Human OCTN2 (SLC22A5) is down-regulated in virus- and nonvirus-mediated cancer.* Cell

Biochem Funct, 2012. **30**(5): p. 419-25.
131. McKinney, N., et al., *EphrinB1 expression is dysregulated and promotes oncogenic signaling in medulloblastoma.* J Neurooncol, 2015. **121**(1): p. 109-18.
132. Cho, H.J., et al., *EphrinB1 interacts with CNK1 and promotes cell migration through c-Jun N-terminal kinase (JNK) activation.* J Biol Chem, 2014. **289**(26): p. 18556-68.
133. Kataoka, H., et al., *Expression profile of EFNB1, EFNB2, two ligands of EPHB2 in human gastric cancer.* J Cancer Res Clin Oncol, 2002. **128**(7): p. 343-8.
134. Liu, Y., et al., *The zinc finger transcription factor ZFHX1A is linked to cell proliferation by Rb-E2F1.* Biochem J, 2007. **408**(1): p. 79-85.
135. Krishnamachary, B., et al., *Hypoxia-inducible factor-1-dependent repression of E-cadherin in von Hippel-Lindau tumor suppressor-null renal cell carcinoma mediated by TCF3, ZFHX1A, and ZFHX1B.* Cancer Res, 2006. **66**(5): p. 2725-31.
136. Nagy, A., et al., *KRAS driven expression signature has prognostic power superior to mutation status in non-small cell lung cancer.* Int J Cancer, 2017. **140**(4): p. 930-937.
137. Hunter, F.W., et al., *The flavoprotein FOXRED2 reductively activates nitro-chloromethylbenzindolines and other hypoxia-targeting prodrugs.* Biochem Pharmacol, 2014. **89**(2): p. 224-35.
138. Liu, X., et al., *Acceleration of pancreatic tumorigenesis under immunosuppressive microenvironment induced by Reg3g overexpression.* Cell Death Dis, 2017. **8**(9): p. e3033.
139. Yin, G., et al., *Reg3g Promotes Pancreatic Carcinogenesis in a Murine Model of Chronic Pancreatitis.* Dig Dis Sci, 2015. **60**(12): p. 3656-68.
140. Lyu, P., et al., *Identification of TWIST-interacting genes in prostate cancer.* Sci China Life Sci, 2017. **60**(4): p. 386-396.
141. Zou, Q., et al., *Clinicopathological features and CCT2 and PDIA2 expression in gallbladder squamous/adenosquamous carcinoma and gallbladder adenocarcinoma.* World J Surg Oncol, 2013. **11**: p. 143.
142. Fischer, S., et al., *Extracellular RNA liberates tumor necrosis factor-alpha to promote tumor cell trafficking and progression.* Cancer Res, 2013. **73**(16): p. 5080-9.
143. Wang, J., et al., *PHF6 regulates cell cycle progression by suppressing ribosomal RNA synthesis.* J Biol Chem, 2013. **288**(5): p. 3174-83.
144. Wang, L., et al., *Comparison of gene expression profiles between primary tumor and metastatic lesions in gastric cancer patients using laser microdissection and cDNA microarray.* World J Gastroenterol, 2006. **12**(43): p. 6949-54.
145. Bell, A., et al., *CpG Island Methylation Profiling in Human Salivary Gland Adenoid Cystic Carcinoma.* Cancer, 2011. **117**(13): p. 2898-2909.
146. Xu, Y., et al., *TMED6-COG8 is a novel molecular marker of TFE3 translocation renal cell carcinoma.* Int J Clin Exp Pathol, 2015. **8**(3): p. 2690-9.
147. Pflueger, D., et al., *Identification of molecular tumor markers in renal cell carcinomas with TFE3 protein expression by RNA sequencing.* Neoplasia, 2013. **15**(11): p. 1231-40.
148. Mapes, J., et al., *Aberrantly high expression of the CUB and zona pellucida-like domain-containing protein 1 (CUZD1) in mammary epithelium leads to breast tumorigenesis.* J Biol Chem, 2018. **293**(8): p. 2850-2864.
149. Leong, C.T., et al., *Silencing expression of UO-44 (CUZD1) using small interfering RNA sensitizes human ovarian cancer cells to cisplatin in vitro.* Oncogene, 2007. **26**(6): p. 870-80.
150. Filippou, P.S., et al., *Kallikrein-related peptidases (KLKs) and the hallmarks of cancer.* Crit Rev Clin Lab Sci, 2016. **53**(4): p. 277-91.
151. Kryza, T., et al., *The kallikrein-related peptidase family: Dysregulation and functions during cancer progression.*

Biochimie, 2016. **122**: p. 283-99.
152. Wang, Z., et al., *Oxidative Stress and Liver Cancer: Etiology and Therapeutic Targets.* Oxid Med Cell Longev, 2016. **2016**: p. 7891574.
153. Perl, A., et al., *Oxidative stress, inflammation and carcinogenesis are controlled through the pentose phosphate pathway by transaldolase.* Trends Mol Med, 2011. **17**(7): p. 395-403.
154. Fu, Y. and F.L. Chung, *Oxidative stress and hepatocarcinogenesis.* Hepatoma Res, 2018. **4**.
155. Bartucci, R., et al., *Vanin 1: Its Physiological Function and Role in Diseases.* Int J Mol Sci, 2019. **20**(16).
156. Berruyer, C., et al., *Vanin-1-/- mice exhibit a glutathione-mediated tissue resistance to oxidative stress.* Mol Cell Biol, 2004. **24**(16): p. 7214-24.
157. Lin, Z.Y. and W.L. Chuang, *Pharmacologic concentrations of ascorbic acid cause diverse influence on differential expressions of angiogenic chemokine genes in different hepatocellular carcinoma cell lines.* Biomed Pharmacother, 2010. **64**(5): p. 348-51.
158. Zhang, B., et al., *The role of vanin-1 and oxidative stress-related pathways in distinguishing acute and chronic pediatric ITP.* Blood, 2011. **117**(17): p. 4569-79.
159. Higgs, M.R., P. Chouteau, and H. Lerat, *'Liver let die': oxidative DNA damage and hepatotropic viruses.* J Gen Virol, 2014. **95**(Pt 5): p. 991-1004.
160. Yang, S.F., et al., *Involvement of DNA damage response pathways in hepatocellular carcinoma.* Biomed Res Int, 2014. **2014**: p. 153867.
161. Eckerdt, F., J. Yuan, and K. Strebhardt, *Polo-like kinases and oncogenesis.* Oncogene, 2005. **24**(2): p. 267-76.
162. Helmke, C., S. Becker, and K. Strebhardt, *The role of Plk3 in oncogenesis.* Oncogene, 2016. **35**(2): p. 135-47.
163. Herzog, C.R., *Chk2 meets Plk3 in damage control.* Cell Cycle, 2002. **1**(6): p. 408-9.
164. Strebhardt, K., *Multifaceted polo-like kinases: drug targets and antitargets for cancer therapy.* Nat Rev Drug Discov, 2010. **9**(8): p. 643-60.
165. Xu, D., W. Dai, and C. Li, *Polo-like kinase 3, hypoxic responses, and tumorigenesis.* Cell Cycle, 2017. **16**(21): p. 2032-2036.
166. Nakagawa, H. and S. Maeda, *Inflammation- and stress-related signaling pathways in hepatocarcinogenesis.* World J Gastroenterol, 2012. **18**(31): p. 4071-81.
167. Sun, B. and M. Karin, *Obesity, inflammation, and liver cancer.* J Hepatol, 2012. **56**(3): p. 704-13.
168. Ringelhan, M., et al., *The immunology of hepatocellular carcinoma.* Nat Immunol, 2018. **19**(3): p. 222-232.
169. Sun, B. and M. Karin, *Inflammation and liver tumorigenesis.* Front Med, 2013. **7**(2): p. 242-54.
170. Aran, G., et al., *CD5L is upregulated in hepatocellular carcinoma and promotes liver cancer cell proliferation and antiapoptotic responses by binding to HSPA5 (GRP78).* FASEB J, 2018. **32**(7): p. 3878-3891.
171. Barcena, C., et al., *CD5L is a pleiotropic player in liver fibrosis controlling damage, fibrosis and immune cell content.* EBioMedicine, 2019. **43**: p. 513-524.
172. Li, Y., et al., *Api6/AIM/Spalpha/CD5L overexpression in alveolar type II epithelial cells induces spontaneous lung adenocarcinoma.* Cancer Res, 2011. **71**(16): p. 5488-99.
173. Li, X., et al., *The presence of IGHG1 in human pancreatic carcinomas is associated with immune evasion mechanisms.* Pancreas, 2011. **40**(5): p. 753-61.
174. Baghdadi, M. and M. Jinushi, *The impact of the TIM gene family on tumor immunity and immunosuppression.* Cell Mol Immunol, 2014. **11**(1): p. 41-8.
175. Zhang, Q., et al., *TIM-4 promotes the growth of non-small-cell lung cancer in a RGD motif-dependent manner.* Br J Cancer, 2015. **113**(10): p. 1484-92.
176. Fang, T., et al., *Orosomucoid 2 inhibits tumor metastasis and is upregulated by CCAAT/enhancer binding protein beta in hepatocellular carcinomas.* Oncotarget, 2015. **6**(18): p. 16106-19.

177. Pineiro, M., et al., *ITIH4 serum concentration increases during acute-phase processes in human patients and is up-regulated by interleukin-6 in hepatocarcinoma HepG2 cells.* Biochem Biophys Res Commun, 1999. **263**(1): p. 224-9.

Figure legends:

Fig. 1 The short form Cirpto-1 (CR-1) mRNA is dominantly expressed in cancer cell lines and clinical tissue specimens of hepatocellular carcinoma (HCC).

(**A**) CR-1 gene and its mRNA structure.

UN-D/UN-B: full-length CR-1 specific primer set; UN-A/UN-B: total CR-1 primer set. The primer couples UN-D/UN-B and UN-A/UN-B yield PCR products of 432bp and 305bp (Fig. 1B, D, F), respectively.

(**B-C**) Representative images of CR-1 isoform expression by RT-PCR (B) and quantification of full-length CR-1 within total CR-1 by semi-quantitative RT-PCR(C) in human HCC cell lines.

(**D-G**) Representative pictures of CR-1 isoform expression (D and F) by RT-PCR, and quantification of full-length CR-1 within total CR-1 by semi-quantitative RT-PCR (E and G) in human HCC clinical tissues pecimens (T/C) and adjacent non-tumorous liver tissues (N/B).

Fig. 2 Expression of CR-1 was elevated in the HCC clinical tissue specimens.

(**A**) Representative pictures of CR-1 transcript levels were examined in HCC clinical specimens (T/C) and matched non-tumorous liver tissues (N/B) by RT-PCR.

(**B**) The T/N ratio of CR-1 mRNA expression shown in Fig. 2A.

The levels of CR-1 transcript were examined in HCC clinical specimens (T/C) and matched non-tumorous liver tissues (N/B) by semi-quantitative RT-PCR.

(**C**) The levels of CR-1 transcript were examined in 65 HCC clinical specimens (T) and 63 adjacent non-HCC liver tissue biopsies(N) by qRT-PCR.

(**D**) The expression levels of CR-1 in HCC clinical specimens (T) and non-cancerous liver tissue biopsies (N) from TCGA datasets.

(**E**) Representative images of CR-1 protein expression in HCC clinical specimens (T) and adjacent non-HCC liver tissue biopsies (N) examined by Western blotting.

(**F**) Representative images of Cirpto-1 expression in HCC clinical specimens and adjacent non-HCC liver tissue biopsies examined by IHC.

(**G**) IHC assay showed that Cirpto-1 expression was markedly higher in the HCC tissue biopsies than that in the non-cancerous liver tissues.

Fig. 3 CR-1 overexpression in liver enhances hepatocyte proliferation after 2/3 partial hepatectomy (PHx).

(**A**) Representative gross pictures of adult RCLG/Alb-Cre mouse (right) and control littermate (left) (5-month-old) fed a normal diet.

(**B**) Body weight of RCLG/Alb-Cre mice and littermate controls at different ages.

(**C**) Relative liver weight of RCLG/Alb-Cre mice vs. littermate controls.

(**D**) Gross morphology of the livers of RCLG/Alb-Cre mouse (right) and control littermate (left)at different ages.

(**E**) Representative histological images of H&E staining of liver sections from control littermates and RCLG/Alb-Cre mice.

(**F**) Hepatocyte proliferation in control littermates and RCLG/Alb-Cre mice, as measured by Ki-67 immunostaining.

(**G**) Hepatocyte proliferation prior to and at indicated time points after PHx in RCLG/Alb-Cre mouse and control littermate, as measured by Ki-67 immunostaining.

(**H**) Ki-67 quantification of hepatocyte proliferation prior to and at indicated time points after PHx in RCLG/Alb-Cre mice (n=3-5) and control littermates(n=3-5).

Fig. 4 CR-1 positively regulated the proliferation, migration and invasion abilities of HCC cells *in vitro*, and CR-1 overexpression promoted tumor growth of HCC cells in nude mice.

(**A**) Western blot analysis of CR-1 expression in vector-expressing (LV-con) and CR-1-expressing (LV-CR-1) BEL-7402 and HepG2 cells.

(**B**) Western blot analysis of CR-1 expression in shSCR-expressing (LV-shSCR) and shCR-1-expressing (LV-shCR-1) BEL-7402 and HepG2 cells.

(**C**) Colony formation assay was performed to test the proliferation ability of CR-1-expressing or shCR-1-expressing HCC cells.

The panels (Fig. S5) show representative pictures of colony formation assay and the panel (Fig. 4C) signify the overall counts of the colonies.

(**D-E**) The motile and invasive activities of CR-1-expressing or shCR-1-expressing BEL-7402 (D) and HepG2 (E) cells based on transwell migration and Boyden invasion assays, respectively.

(**F**) Representative picture of nude mice bearing a human HCC subcutaneous xenografts.

(**G**) Representative picture of tumors formed.

(**H**) Growth curve of tumor volumes.

(**I**) Tumors were weighted.

(**J-K**) BrdU-stained sections of transplanted tumors formed by BEL-7402 cells.

As mentioned in Materials and methods section, nude mice were subcutaneously implanted with vector- and CR-1-expressing BEL-7402 cells. The percentages of BrdU-positive cancer cells were calculated by the total number of BrdU-positive cells over total number of cancer cells.

Fig. 5 Liver-specific overexpression of CR-1 gene in transgenic mice activates HCC-related common signaling pathways.

(**A**) Representative Western blot analysis of the indicated proteins in CR-1-expressing or shCR-1-expressing BEL-7402 and HepG2 cells.

(**B**) Representative immunoblotting showing the indicated protein levels in the liver of RCLG/Alb-Cre mice.

(**C**) The relative mRNA levels of IL-1, IL-6, Notch1 and TGF-β1 in the liver of RCLG/Alb-Cre mice based on qRT-PCR assay.

Fig. 6 Microarray revealed the altered expression of genes involved in HCC oncogenesis in the liver of RCLG/Alb-Cre mice.

(**A**) Class comparison and hierarchical clustering of differentially expressed hepatocarcinogenesis-related genes between RCLG/Alb-Cre and control mouse liver.
Tg-1, Tg-2 and Tg-5 represented the total RNA (used in microarray experiment) isolated from the livers of three 4-month-old RCLG/Alb-Cre transgenic mice, while cc represented the pooled total RNA (used in microarray experiment) isolated from the livers of three control littermates. Equal amounts of total RNA from each control liver vole were pooled to prepare cc. Tg-1 vs cc: Tg-1 compared to pooled cc; Tg-2 vs cc: Tg-2 compared to pooled cc; Tg-5 vs cc: Tg-5 compared to pooled cc. Only genes showing a fold change of more than 2 and a t test P value of less than 0.05 were included in the analysis. Red indicates increased expression; blue indicates reduced expression. Other details as in Fig. S7.
(**B-D**) qRT-PCR validated microarray-derived data on the increased or decreased mRNA expression of the indicated HCC oncogenesis-related genes in RCLG/Alb-Cre mouse liver.

Fig. 7 HCC specimen-derived data validated the altered expression of genes found in the liver of RCLG/Alb-Cre mice

(**A-B**) The expression levels of CR-1 in HCC clinical specimens (T) and non-cancerous liver tissue biopsies (N) derived from NCBIGEO datasets (GSE14520 and GSE25097).
(**C-D**) qRT-PCR analysis of the expression of the indicated genes (selected from Fig. 6A-D) in HCC primary tumor (T) and matched nontumorous liver (N) tissues.
(**E**) Representative images of PDK4 expression in HCC clinical specimens and adjacent non-HCC liver tissue biopsies examined by IHC.
(**F**) IHC assay showed that PDK4 expression was markedly lower in the HCC tissue biopsies than that in the non-cancerous liver tissues.

Figures

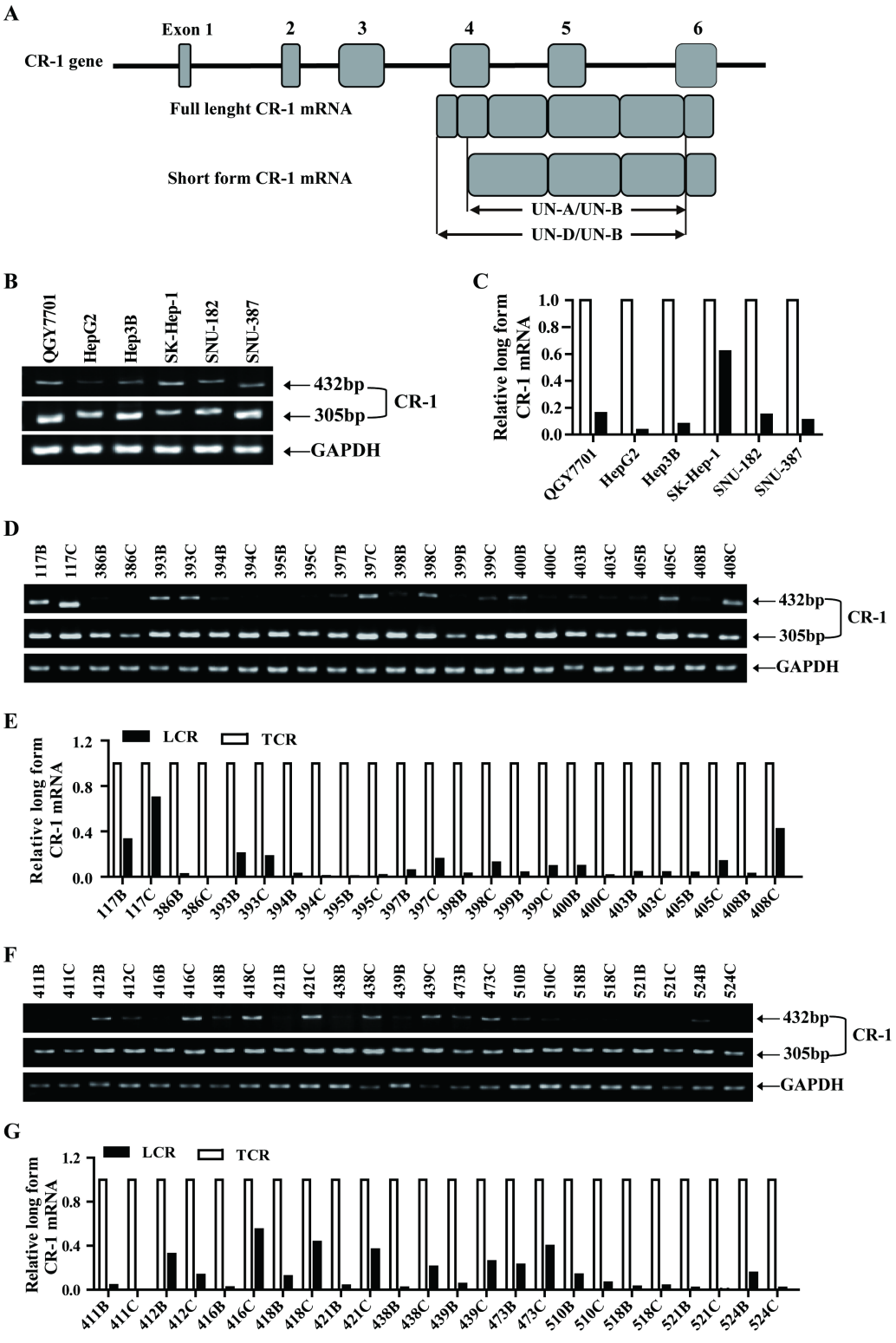

Figure 1

The short form Cirpto-1 (CR-1) mRNA is dominantly expressed in cancer cell lines and clinical tissue specimens of hepatocellular carcinoma (HCC). (A) CR-1 gene and its mRNA structure. UN-D/UN-B: full-length CR-1 specific primer set; UN-A/UN-B: total CR-1 primer set. The primer couples UN-D/UN-B and UN-

A/UN-B yield PCR products of 432bp and 305bp (Fig. 1B, D, F), respectively. (B-C) Representative images of CR-1 isoform expression by RT-PCR (B) and quantification of full-length CR-1 within total CR-1 by semi-quantitative RT-PCR(C) in human HCC cell lines. (D-G) Representative pictures of CR-1 isoform expression (D and F) by RT-PCR, and quantification of full-length CR-1 within total CR-1 by semi-quantitative RT-PCR (E and G) in human HCC clinical tissues pecimens (T/C) and adjacent non-tumorous liver tissues (N/B).

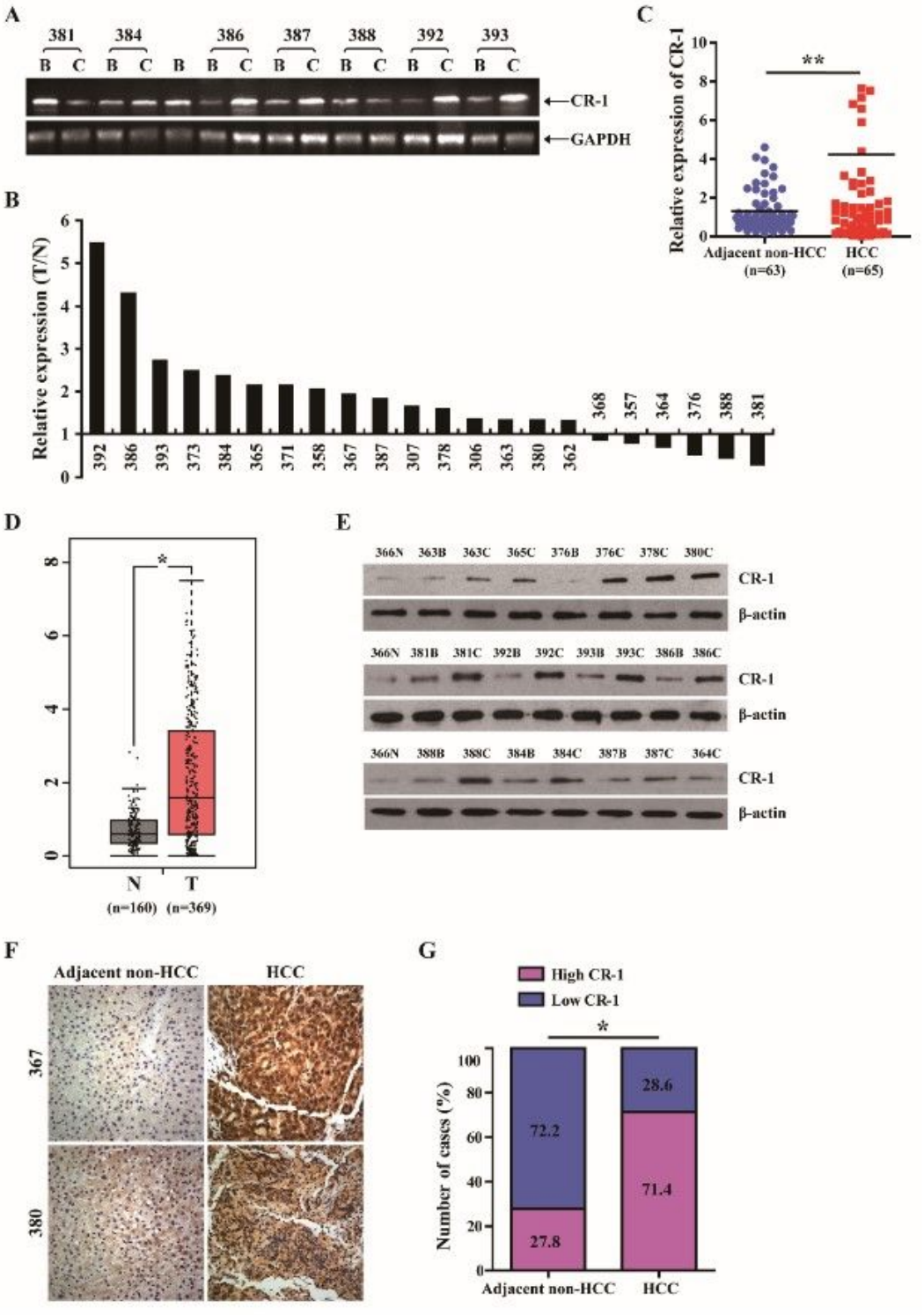

Figure 2

Expression of CR-1 was elevated in the HCC clinical tissue specimens. (A) Representative pictures of CR-1 transcript levels were examined in HCC clinical specimens (T/C) and matched non-tumorous liver tissues (N/B) by RT-PCR. (B) The T/N ratio of CR-1 mRNA expression shown in Fig. 2A. The levels of CR-1 transcript were examined in HCC clinical specimens (T/C) and matched non-tumorous liver tissues (N/B) by semi-quantitative RT-PCR. (C) The levels of CR-1 transcript were examined in 65 HCC clinical specimens (T) and 63 adjacent non-HCC liver tissue biopsies(N) by qRT-PCR. (D) The expression levels of CR-1 in HCC clinical specimens (T) and non-cancerous liver tissue biopsies (N) from TCGA datasets. (E) Representative images of CR-1 protein expression in HCC clinical specimens (T) and adjacent non-HCC liver tissue biopsies (N) examined by Western blotting. (F) Representative images of Cirpto-1 expression in HCC clinical specimens and adjacent non-HCC liver tissue biopsies examined by IHC. (G) IHC assay showed that Cirpto-1 expression was markedly higher in the HCC tissue biopsies than that in the non-cancerous liver tissues.

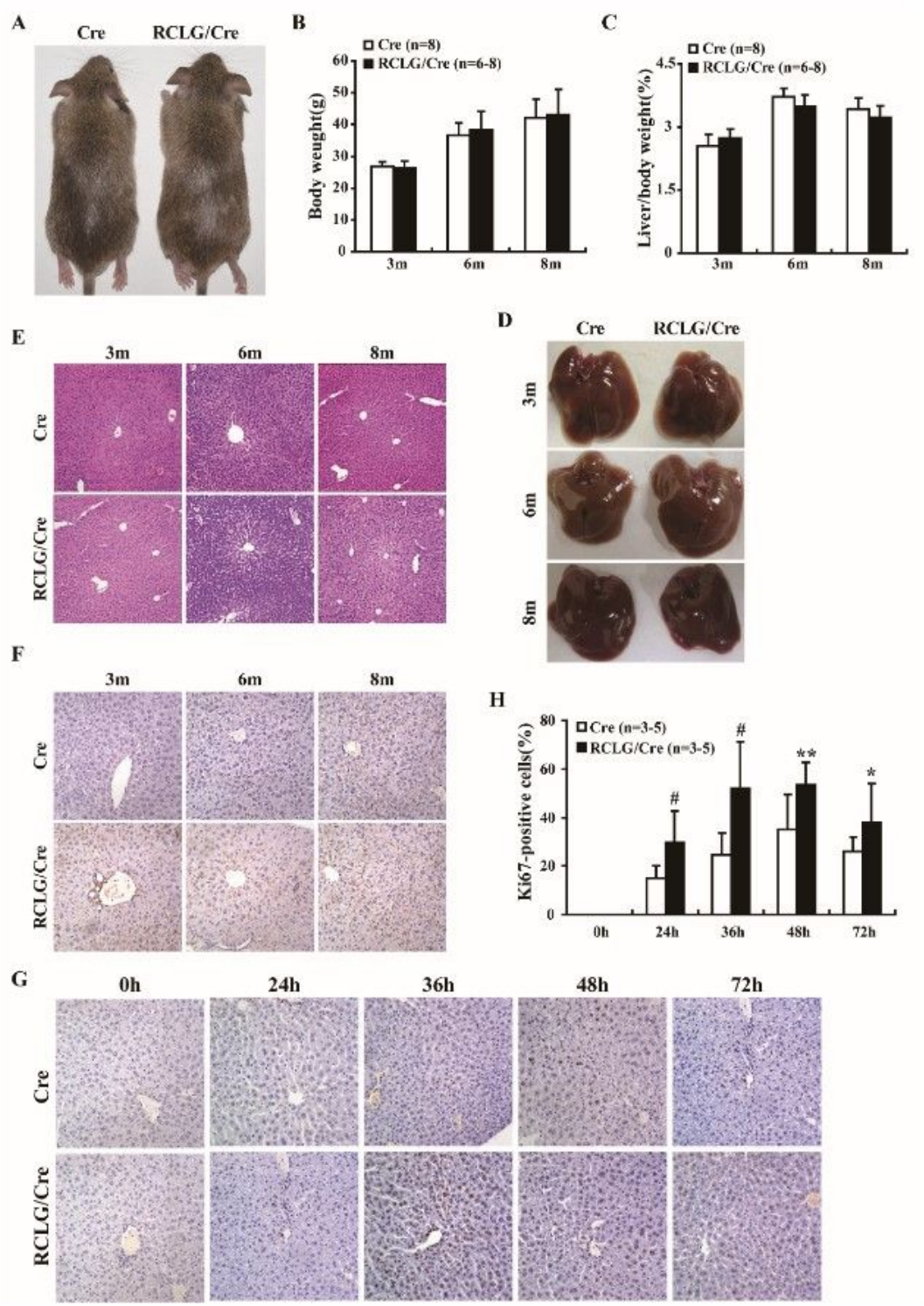

Figure 3

CR-1 overexpression in liver enhances hepatocyte proliferation after 2/3 partial hepatectomy (PHx). (A) Representative gross pictures of adult RCLG/Alb-Cre mouse (right) and control littermate (left) (5-month-old) fed a normal diet. (B) Body weight of RCLG/Alb-Cre mice and littermate controls at different ages. (C) Relative liver weight of RCLG/Alb-Cre mice vs. littermate controls. (D) Gross morphology of the livers of RCLG/Alb-Cre mouse (right) and control littermate (left)at different ages. (E) Representative histological

images of H&E staining of liver sections from control littermates and RCLG/Alb-Cre mice. (F) Hepatocyte proliferation in control littermates and RCLG/Alb-Cre mice, as measured by Ki-67 immunostaining. (G) Hepatocyte proliferation prior to and at indicated time points after PHx in RCLG/Alb-Cre mouse and control littermate, as measured by Ki-67 immunostaining. (H) Ki-67 quantification of hepatocyte proliferation prior to and at indicated time points after PHx in RCLG/Alb-Cre mice (n=3-5) and control littermates(n=3-5).

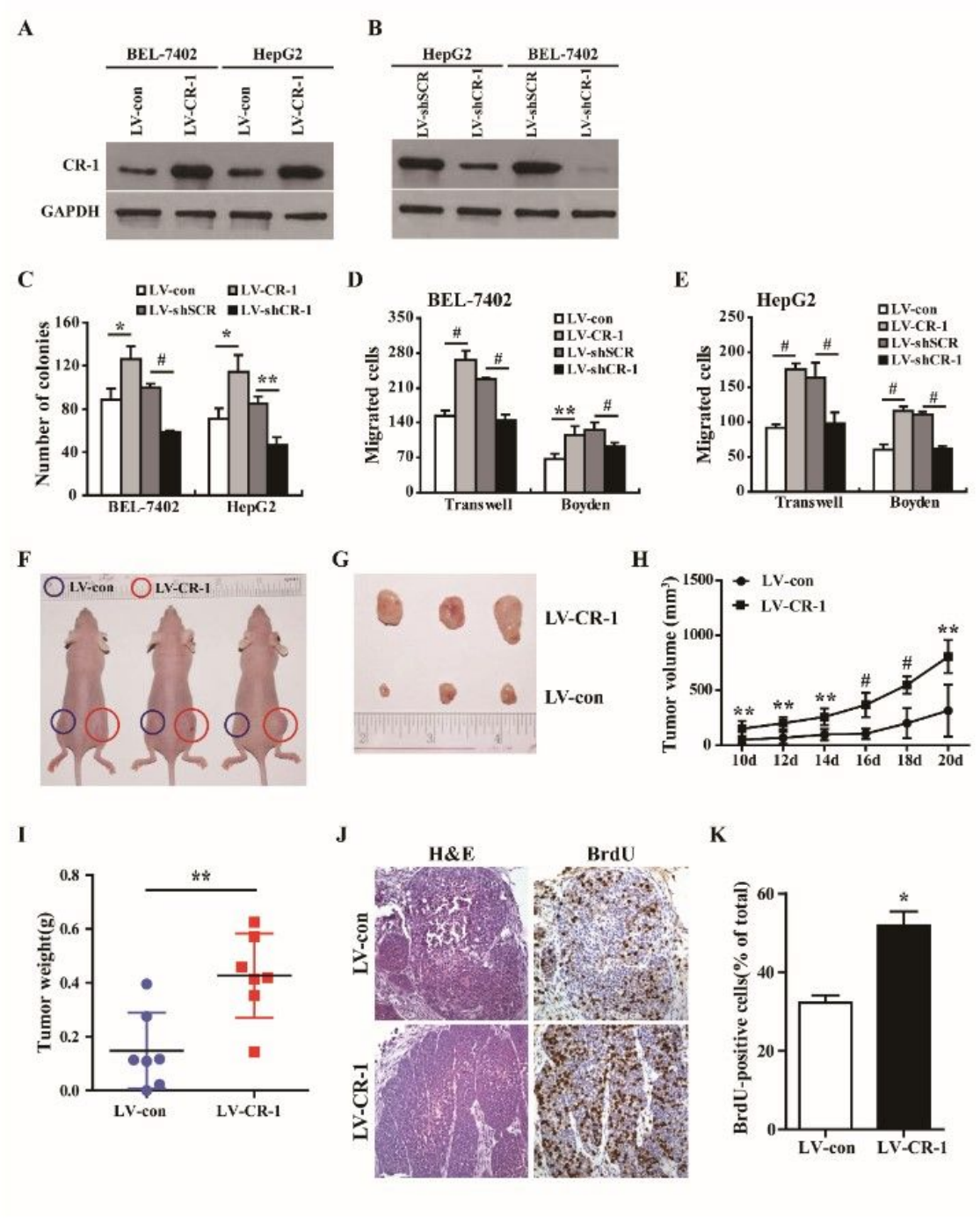

Figure 4

CR-1 positively regulated the proliferation, migration and invasion abilities of HCC cells in vitro , and CR-1 overexpression promoted tumor growth of HCC cells in nude mice. (A) Western blot analysis of CR-1 expression in vector-expressing (LV-con) and CR-1-expressing (LV-CR-1) BEL-7402 and HepG2 cells. (B) Western blot analysis of CR-1 expression in shSCR-expressing (LV-shSCR) and shCR-1-expressing (LV-shCR-1) BEL-7402 and HepG2 cells. (C) Colony formation assay was performed to test the proliferation ability of CR-1-expressing or shCR-1-expressing HCC cells. The panels (Fig. S5) show representative pictures of colony formation assay and the panel (Fig. 4C) signify the overall counts of the colonies. (D-E) The motile and invasive activities of CR-1-expressing or shCR-1-expressing BEL-7402 (D) and HepG2 (E) cells based on transwell migration and Boyden invasion assays, respectively. (F) Representative picture of nude mice bearing a human HCC subcutaneous xenografts. (G) Representative picture of tumors formed. (H) Growth curve of tumor volumes. (I) Tumors were weighted. (J-K) BrdU-stained sections of transplanted tumors formed by BEL-7402 cells. As mentioned in Materials and methods section, nude mice were subcutaneously implanted with vector- and CR-1-expressing BEL-7402 cells. The percentages of BrdU-positive cancer cells were calculated by the total number of BrdU-positive cells over total number of cancer cells.

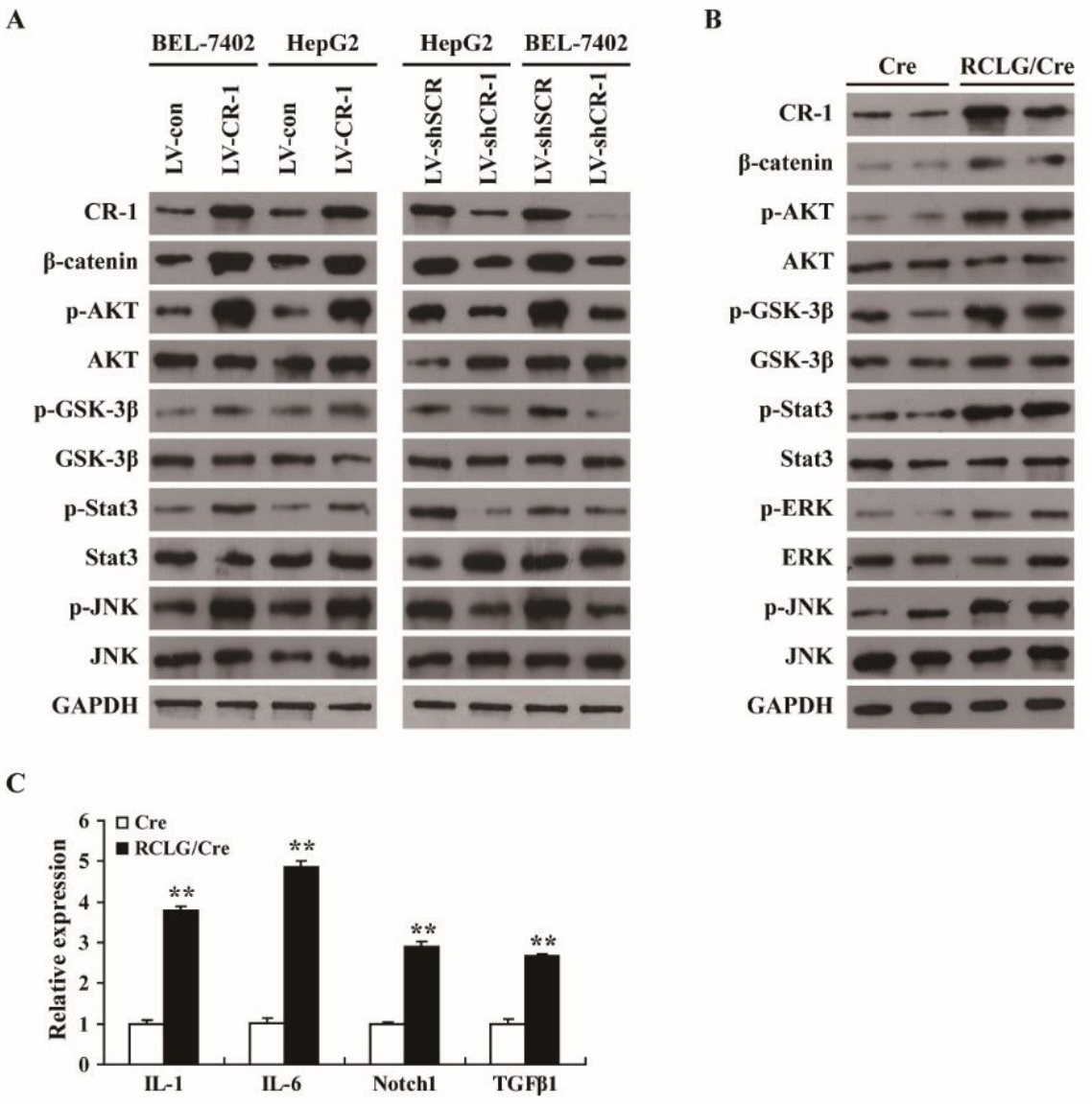

Figure 5

Liver-specific overexpression of CR-1 gene in transgenic mice activates HCC-related common signaling pathways. (A) Representative Western blot analysis of the indicated proteins in CR-1-expressing or shCR-1-expressing BEL-7402 and HepG2 cells. (B) Representative immunoblotting showing the indicated protein levels in the liver of RCLG/Alb-Cre mice. (C) The relative mRNA levels of IL-1, IL-6, Notch1 and TGF-β1 in the liver of RCLG/Alb-Cre mice based on qRT-PCR assay.

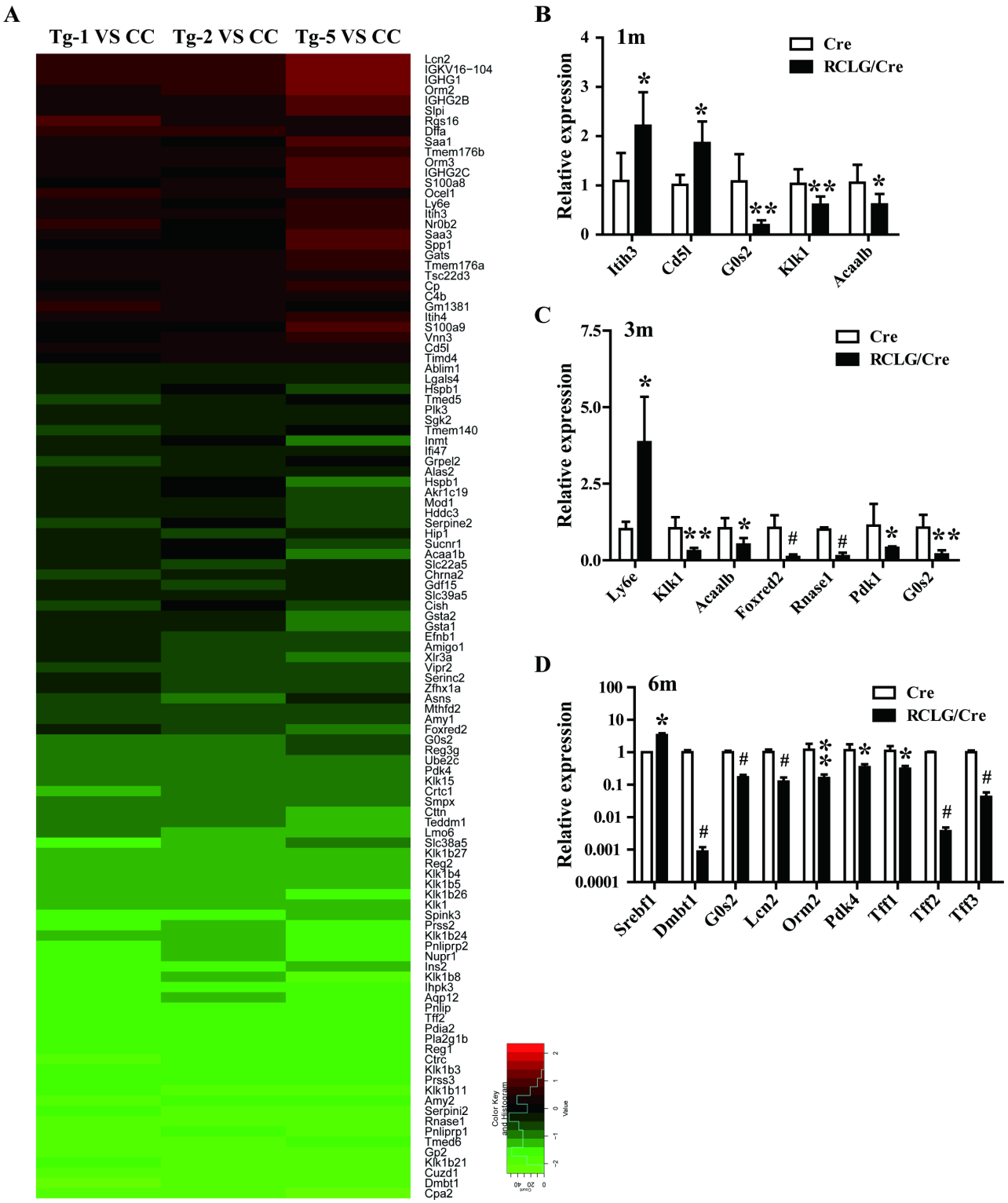

Figure 6

Microarray revealed the altered expression of genes involved in HCC oncogenesis in the liver of RCLG/Alb-Cre mice. (A) Class comparison and hierarchical clustering of differentially expressed hepatocarcinogenesis-related genes between RCLG/Alb-Cre and control mouse liver. Tg-1, Tg-2 and Tg-5 represented the total RNA (used in microarray experiment) isolated from the livers of three 4-month-old RCLG/Alb-Cre transgenic mice, while cc represented the pooled total RNA (used in microarray experiment)

isolated from the livers of three control littermates. Equal amounts of total RNA from each control liver vole were pooled to prepare cc. Tg-1 vs cc: Tg-1 compared to pooled cc; Tg-2 vs cc: Tg-2 compared to pooled cc; Tg-5 vs cc: Tg-5 compared to pooled cc. Only genes showing a fold change of more than 2 and a t test P value of less than 0.05 were included in the analysis. Red indicates increased expression; blue indicates reduced expression. Other details as in Fig. S7. (B-D) qRT-PCR validated microarray-derived data on the increased or decreased mRNA expression of the indicated HCC oncogenesis-related genes in RCLG/Alb-Cre mouse liver.

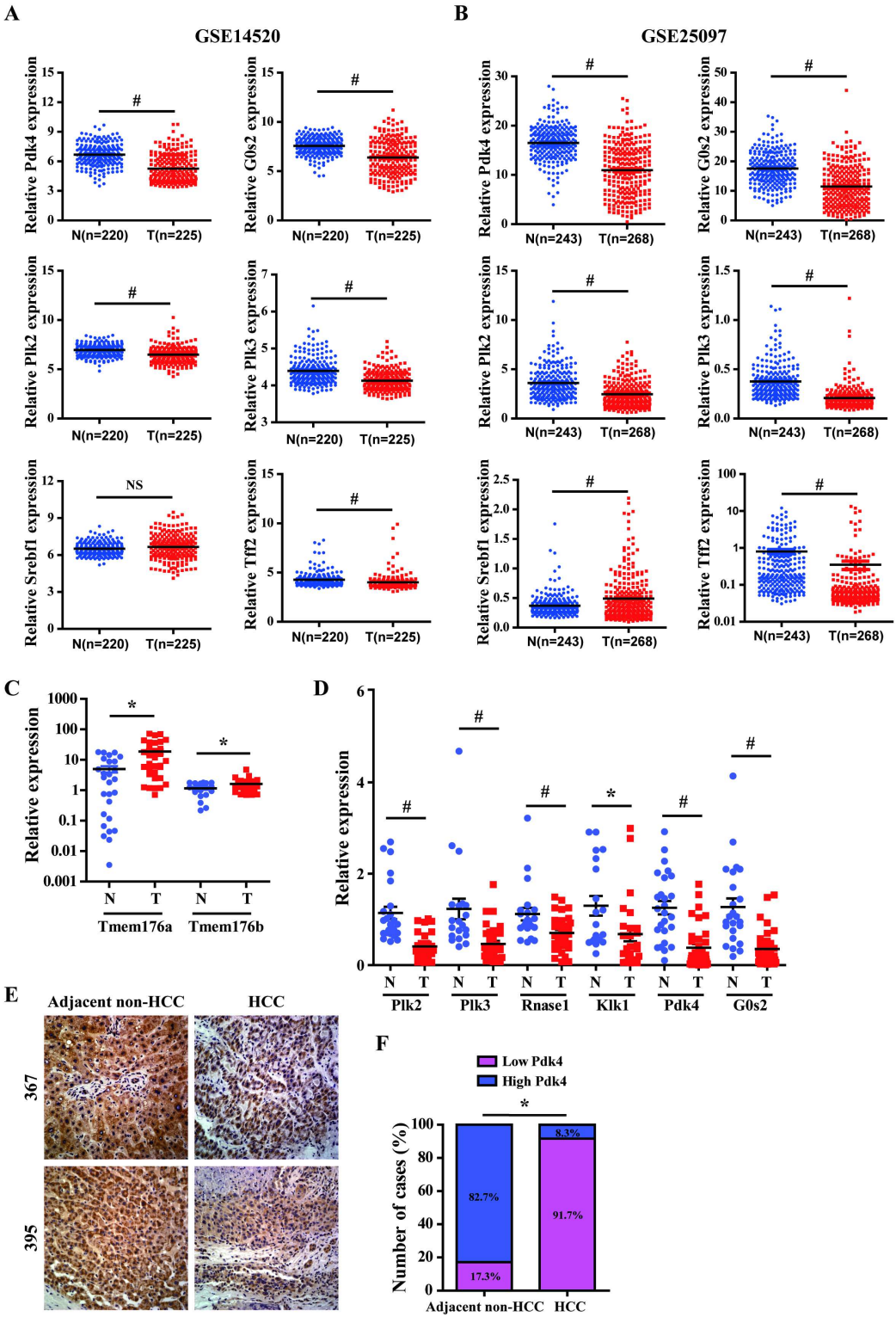

Figure 7

HCC specimen-derived data validated the altered expression of genes found in the liver of RCLG/Alb-Cre mice (A-B) The expression levels of CR-1 in HCC clinical specimens (T) and non-cancerous liver tissue biopsies (N) derived from NCBIGEO datasets (GSE14520 and GSE25097). (C-D) qRT-PCR analysis of the expression of the indicated genes (selected from Fig. 6A-D) in HCC primary tumor (T) and matched nontumorous liver (N) tissues. (E) Representative images of PDK4 expression in HCC clinical specimens and adjacent non-HCC liver tissue biopsies examined by IHC. (F) IHC assay showed that PDK4 expression was markedly lower in the HCC tissue biopsies than that in the non-cancerous liver tissues.

Supplementary Files

This is a list of supplementary files associated with this preprint. Click to download.

- CR1Supplementaryfigures.pdf
- TableS1.pdf
- TableS6.pdf
- TableS4.pdf
- TableS3.pdf
- TableS2.pdf
- TableS5.pdf
- TableS7.pdf
- TableS8.pdf